ABSTRACT

MAGNETICALLY ASSISTED IMPACTION MIXING OF NANOSIZE PARTICLES

by
James V. Scicolone

Magnetically assisted impaction mixing (MAIM) is a novel dry mixing technique, which can be used to mix nanoparticles. Mixing of nanoparticles is usually conducted in solvent-based mixing techniques. The solvents used in these techniques are usually organic, which can be expensive and harmful to the environment. MAIM creates homogeneous nanoparticle mixtures while eliminating conditioning and drying steps associated with wet mixing techniques. To create the best mixing quality of nanoparticles, MAIM was optimized by studying the effects of magnet-to-sample ratio, time, magnet size, and constituents of the mixture. The results were then compared with other well-known mixing techniques.

To characterize the nanoparticle mixtures on a micron scale, a field emission scanning electron microscope and energy dispersive x-ray spectroscopy were used at 5000 times magnification. The results obtained from images and compound percent point analysis shows that the new MAIM technique produces a mixture quality of nanoparticles similar to supercritical sonication mixing.

MAGNETICALLY ASSISTED IMPACTION MIXING OF NANOSIZE PARTICLES

by
James V. Scicolone

A Thesis
Submitted to the Faculty of
New Jersey Institute of Technology
in Partial Fulfillment of the Requirements for the Degree of
Master of Science in Chemical Engineering

Otto H. York Department of Chemical Engineering

January 2008

APPROVAL PAGE

MAGNETICALLY ASSISTED IMPACTION MIXING OF NANOSIZE PARTICLES

James V. Scicolone

Dr. Rajesh N. Dave. Dissertation Advisor — Date
Distinguished Professor of Chemical Engineering, NJIT

Dr. Robert Pfeffer, Committee Member — Date
Distinguished Professor of Chemical Engineering (Emeritus), NJIT

Dr. Norman Loney, Committee Member — Date
Professor of Chemical Engineering, NJIT

BIOGRAPHICAL SKETCH

Author: James Vincent Scicolone

Degree: Master of Science

Date: January 2008

Undergraduate and Graduate Education:

- Masters of Science in Chemical Engineering,
  New Jersey Institute of Technology, Newark, NJ, USA, 2008

- Bachelor of Science in Chemical Engineering,
  Penn State University, Pennsylvania, USA, 2005

Major: Chemical Engineering

Presentations and Publications:

James V. Scicolone, Alexandre Ermoline, and Rajesh N. Dave, "Mechanically Assisted Impaction Mixing of Submicron Particles," in preparation.

Ganesh Sanganwar, Alexandre Ermoline, James Scicolone, Rajesh N. Dave, Ram B. Gupta, "Environmentally Benign Nanomixing by Sonication in Supercritical CO_2" in preparation.

James V. Scicolone, Alexandre Ermoline, and Rajesh N. Dave, "Mechanically Assisted Impaction Mixing of Nanosize Particles," 2007 AIChE Annual Meeting, Salt Lake City, Utah, November 5, 2007.

James V. Scicolone, Peter K. Davis, Ronald P. Danner, and J. Larry Duda, "Solubility and diffusivity of solvents by packed column inverse gas chromatography," Polymer, Vol. 47, pp. 5364-5370, 2006.

James V. Scicolone, Peter K. Davis, Ronald P. Danner, and J. Larry Duda, "Measurement of Diffusion and Partition Coefficients for Solvents in Polyethylene Pellets by Packed Column Inverse Gas Chromatography," ACS 36th Middle Atlantic Regional Meeting (MARM) 2003, Princeton, NJ, June 2003.

This thesis is dedicated to my family, and their continued devotion

"One of the symptoms of an approaching nervous breakdown
is the belief that one's work is terribly important."
- Bertrand Russell

ACKNOWLEDGMENT

I would like to express my deepest appreciation to Dr. Rajesh Dave, who not only served as my research supervisor, but also introduced me to the particle field. His valuable knowledge and dedication providing valuable insight, and intuition, but also constantly gave me support, encouragement, and reassurance. Special thanks are given to Dr. Robert Pfeffer and Dr. Norman Loney for actively participating in my committee.

I would also like to acknowledge the financial support Dr. Rajesh Dave provided for me from the National Science Foundation IGERT Award (DMI-0506722). I would also like to acknowledge the financial support Dr. Robert Pfeffer provided for me from the National Science Foundation NNCS Award (DMI-0210400).

I would like to thank my family: my parents Salvatore and Lori; my brother Michael; my grandparents Gioacchino and Vincenza; my aunt Lillie; and my cousins Vivi, John, and Priscilla. Your achievements and sacrifices have molded me into the man I am, and I deeply thank you for all you have done.

I wish to thank Dr. Alexandre Ermoline for his assistance in the laboratory, knowledge, and guidance through this process. Many of my fellow graduate students in the Chemical Engineering Department are deserving of recognition for their support. Finally, I would like to thank Ganesh Sanganwar, Laila Jallo, and Lauren Beach for their assistance with some of the experiments.

TABLE OF CONTENTS

TABLE OF CONTENTS

LIST OF TABLES

LIST OF FIGURES

CHAPTER 1

INTRODUCTION

1.1 Objective

The objective of this thesis is to improve and explore the homogeneity of nanoparticle mixtures obtained using a novel, dry mixing technique. Magnetically Assisted Impaction Mixing (MAIM) is an environmentally benign dry mixing technique that does not require any solvents, conditioning steps, or subsequent drying time. Characterizing mixtures requires the analysis on the micron range, while including a larger bulk analysis. An in depth study characterizing changes in the magnets and time shows that MAIM can produce a homogeneous mixture on the submicron scale.

1.2 Background

This thesis addresses the topic of mixing nanoparticles using MAIM, and characterizing the mixtures using a field emission scanning electron microscope (FESEM) and energy dispersive x-ray spectroscopy (EDS). Generally, the mixing of particles is used predominantly in industry, but most cases involve non-cohesive, spherical particles[1, 2] and they are rarely on the submicron scale. Nanoparticles fall under the category of cohesive particles because they are usually in agglomerated forms.

When particles reach the nano-scale level, the surface area to volume ratio increases greatly, and there are more atoms located near the surface of the nanoparticle. Particle size plays a major role on the forces acting upon the particle. Since gravitational forces are proportional to the cube of the particle diameter, small changes in particle size

have a pronounced effect on the gravitational force. With the higher percentage of atoms found at the surface of the nanoparticle, intermolecular forces become more significant. Capillary forces, immobile liquid bridges, electrostatic attraction, and van der Waals attractive forces are the three major intermolecular forces to be considered. Capillary bonds and liquid bridges, which arise due to the precipitation of liquid on the surface of the particles, are influential in high humidity environments. If the humidity level is controlled, these forces become less important. Electrostatic attractive forces are considered negligible when compared to van der Waals forces.

Van der Waals forces are proportional to the diameter of the particle. For particle sizes at, and below, the micron-scale, van der Waals attractive forces become significantly stronger than the gravitational forces acting on the particle. Since the attractive forces are more significant, nanoparticles tend to form aggregates that form agglomerates that can become larger than one hundred microns in diameter. The agglomerates are loosely compact and have large void areas, generally in excess of 99% void. New properties from these nanoparticles appear on both nanoparticle coating and nano-composites due to the particles approaching the size of molecules and atoms. Unique properties of nano-composites arise from the interaction of different constituents at the interfaces at the nano scale[3-7]. A few of these properties include enhancements in chemical catalysts, ware resistance, oxidation resistance, thermal resistance, and corrosion resistance[8].

With recent attention and research surrounding nanoparticles, the need to develop new methods of mixing submicron particles is increasingly necessary. Conventional dry mixing methods like tumbling or fluidized bed mixing[9] do not work for mixing of

nanoparticles because there are not enough forces to break up the agglomerates. The mixing would only be on the level of the size of the agglomerates. To mix on a submicron scale, forces and mixing motion are required to deagglomerate and then mix the particles at sub-micron scales. Industries have moved toward wet mixing because the solvents have a higher viscosity and can penetrate into the agglomerate void spaces, making the process of deagglomeration easier. However, the solvents, which tend to be organic solvents, can be expensive and are harmful to the environment[10]. There are other disadvantages associated with wet mixing processes, such as conditioning steps and downstream drying time. During the drying time, segregation occurs which adversely affects the homogeneity of the mixture. The New Jersey Center for Engineered Particulates (NJCEP) group uses multiple dry mixing techniques that focus on deagglomeration and mixing of nanoparticles by creating high shear forces.[1]

Analyzing a mixture of nanoparticles is difficult due to poor spatial resolution. Analysis methods have been determined for particles with primary particle sizes greater than ten microns. Many methods require much sampling and can be very time consuming. Field emission scanning electron microscopy (FESEM) and energy dispersive x-ray spectroscopy (EDS) are used to analyze the mixtures of nanoparticles. Previous research using MAIM[1,2] have shown poor mixing levels on the micron level, thus analysis in this thesis focused on the micron level. However, through the course of this research, FESEM and EDS images have shown that the mixing from MAIM can produce homogeneity below the resolution level of these analysis devices. Mixing on the submicron scale can be inferred from MAIM mixing, and future study analysis methods require transmission electron microscope

1.3 Magnetically Assisted Impaction Mixing

MAIM is a dry mixing technique developed at the laboratory of NJCEP at New Jersey Institute of Technology in Newark, New Jersey. MAIM is based on the magnetically assisted impaction coater (MAIC)[5]. The MAIC is patented by Aveka (Minnesota, USA). Dry mixing methods not only eliminate the need to use harmful solvents associated with wet mixing, but also eliminate conditioning or drying processes.

Figure 1 is a schematic of the MAIM apparatus. The weighed components of nanoparticles and magnetic particles are charged in a central container. The magnetic particles are composed of barium ferrite and are coated with polyurethane to prevent any contamination from the magnetic particles onto the mixture. The container with the constituents is surrounded by a circular electromagnetic coil. A fan is connected underneath the coil to prevent any overheating. The device is controlled by a Variac 140V variable transformer connected to alternating current.

A magnetic field is created from the surrounding electromagnetic coil and the magnetic particles undergo agitation. The magnetic particles undergo rotational and translational motion, inside the container, creating a fluidized state for the nanoparticles. Magnetic particles collide with the agglomerates of nanoparticles, and other magnetic particles or the walls of the container, passing on the energy from the generated momentum. The collisions between magnetic particles and the agglomerates contain enough energy to deagglomerate the nanoparticle agglomerates and promote mixing.

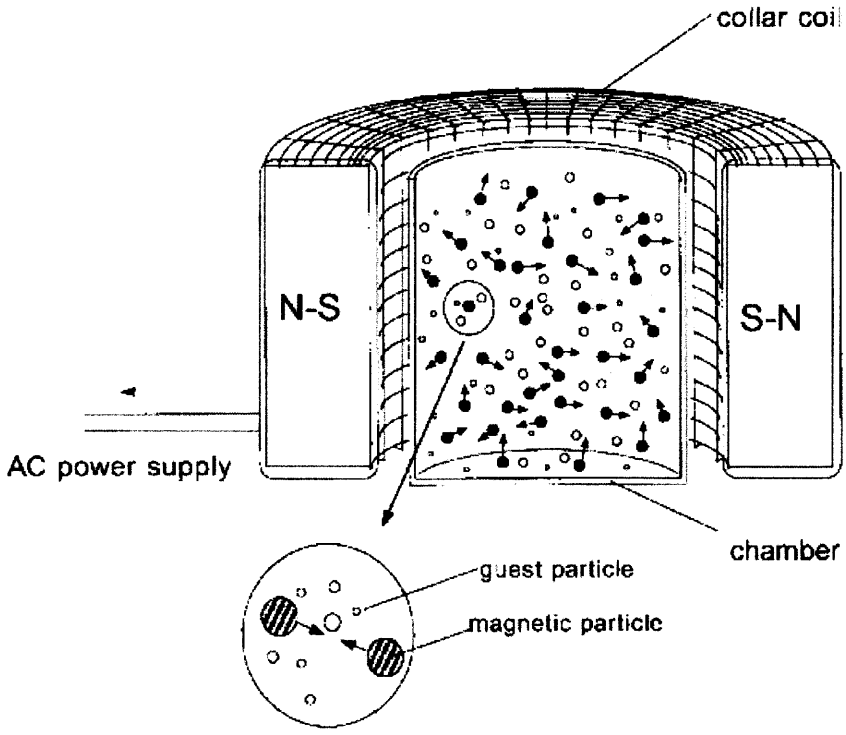

Figure 1 Experimental Setup Schematic of MAIM.[2]

CHAPTER 2
EXPERIMENTAL DETAILS

2.1 Materials

The research focused on nanopowders of fumed silica Aerosil® R974 and Aerosil® R972 along with Aeroxide® TiO_2 P25 and Aeroxide® Alu C. The Aerosil® particles are hydrophobic and the Aeroxide® particles are hydrophilic. All samples are provided by Degussa Corporation. Further nanoparticle information is presented in Table 2.1. Silica Aerosil® R974 and titania Aeroxide® P25 were the primary particles studied with MAIM. All nanoparticles were sieved to remove any groupings of agglomerates larger than 500 microns.

The barium ferrite magnetic particles, purchased from AVEKA INC, are coated with polyurethane to prevent contamination and to limit the mixture's retention. The magnetic particles are in three size ranges of 2360 to 1700 microns, 1400 to 850 microns, and 1000 to 600 microns. The majority of experiments are carried out with the 1400 to 850 microns magnetic particles.

Once the mixing is complete, the magnetic particles are sieved from the nanoparticles. Two 13 millimeter sized tablets are pressed under constant pressure of 16,000 lb/in^2 to create a uniform packed density. The magnetic particles can be cleaned and reused. Materials are affordable allowing the process to be scaled up with relative ease.

Table 2 Nanoparticle Properties

Material	Primary Particle Size (nm)	Surface Area (m^2/g)	Property
Aerosil® R974	12	200	Hydrophobic
Aeroxide® TiO_2 P25	21	50	Hydrophilic
Aeroxide® Alu C	13	100	Hydrophilic
Aerosil® R972	16	130	Hydrophobic

2.2 Analytical Equipment

A LEO Field Emission Scanning Electron Microscope (FESEM) equipped with an Oxford UTW X-ray detector is used to analyze the mixtures. The spectrum was obtained under an accelerating voltage of 15 keV and a working distance of approximately 8 mm. First, a thin coating of electrically conducting carbon is deposited by vacuum sputter coating onto the sample. Coating samples prevent the accumulation of static electric fields on the specimen and improves the contrast. Contrast is important for the qualitative analysis presented in Chapter 3.

The FESEM detects secondary electrons created from the interaction between the incident beam and the sample. The secondary electrons are low energy, originating only a few nanometers from the surface. Once the electrons are detected, the resulting signal is turned into a digital image. The brightness of the signal depends on the number of secondary electrons reaching the detector. Brightness also depends on the atomic number of the material being analyzed, such that a sample with a larger atomic number will appear brighter.

Through secondary electrons images, elements that have a large enough atomic number difference will appear either lighter or darker by contrast. The contrast is evident with mixtures containing constituents of any silica (Z=14) and titania (Z=22), but is not visible to mixtures with constituents of silica (Z=14) and alumina (Z=13). Thus, mixtures of silica Aerosil® R974 and Aeroxide® titania P25 were used. The secondary electrons images serve as a method to characterize the homogeneity of the mixture on the surface of a tablet. Two locations on each of the two tablets were imaged, at a 5000-x magnification. Figure 2.1 is a secondary electron image from the FESEM.

Energy dispersive X-ray spectroscopy (EDS) is used for elemental identification and is a useful tool for characterizing mixing quality. The EDS has a resolution of approximately 1 micron. EDS characterizes individual elements due to their unique electronic structure and response to the electromagnet waves. An elemental mapping and a point analysis provides homogeneity images and composition of the material. The EDS elemental mapping separates the elements into individual images. Figure 2.2 contains a secondary electron image from the FESEM and an elemental mapping of silicon, titanium, and oxygen at the same location. The bright areas on the image represent a high concentration of the specific element. An elemental mapping is obtained at each of the four locations per mixture. The EDS point analysis provides compound percent data at any desired point. One hundred points of compound percent is collected from a ten by ten grid covering the area of the image, for each image, totaling four-hundred points per mixture. Figure 2.3 is a representation of the ten by ten grid used to collect compound percentage data.

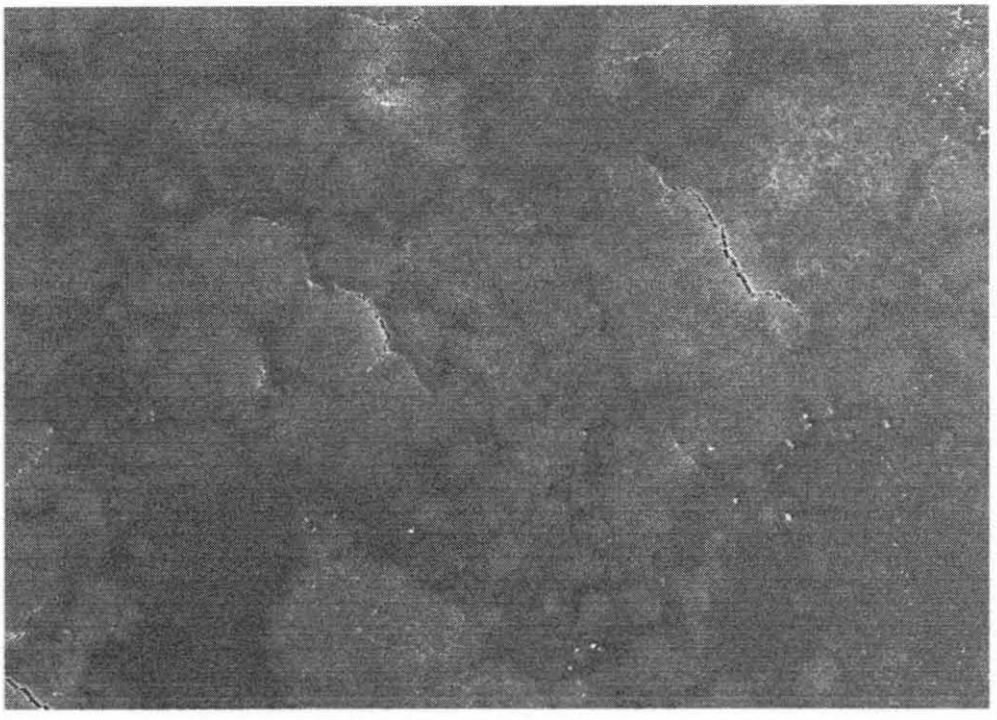

Figure 2.1 Secondary electron image.

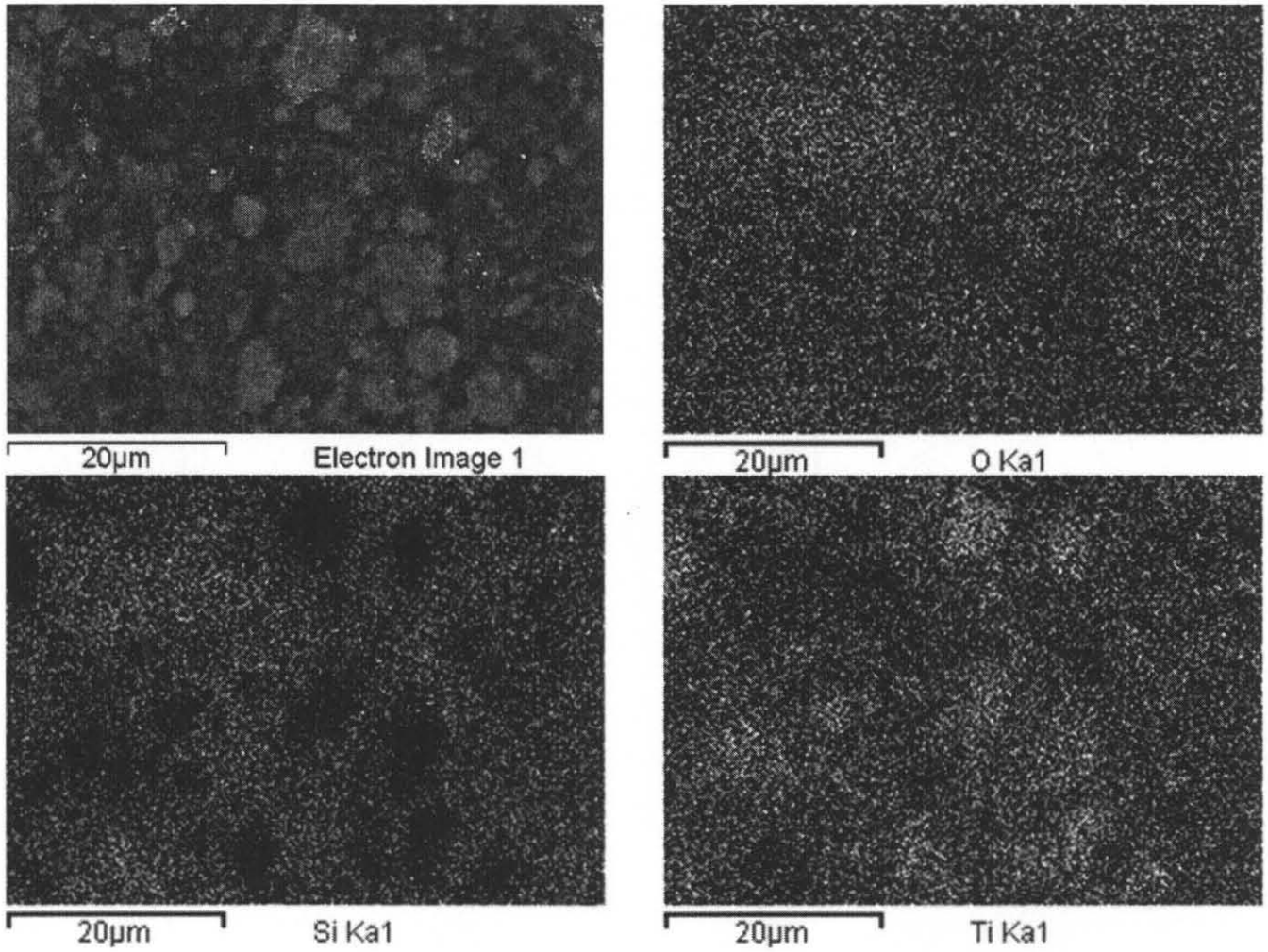

Figure 2.2 EDS mapping. Secondary electron Image (top left), oxygen elemental mapping (top right), silicon elemental mapping (bottom left), titanium elemental mapping (bottom right

Figure 2.3 Secondary electron image with ten by ten-point grid.

CHAPTER 3

ANALYSIS

Chapter 3 contains details of how the qualitative and quantitative data are collected. Qualitative data are collected using the secondary electron images, obtained from SEM, and X-ray elemental mapping images, obtained from EDS. Quantitative analysis is obtained from X-ray compound percent point analysis obtained from the EDS.

3.1. Statistical Analysis

Four hundred total points are obtained for each mixture analyzing approximately 1 to 2 microns. The points are grouped and the values for average (μ), variance (σ^2), and standard deviation (σ), represented by Equations 3.1 through 3.3, are calculated from the compound percent data.

$$\mu = \frac{\sum_{i}^{n} x_i}{n} \tag{3.1}$$

$$\sigma^2 = \frac{\left(\sum_{i}^{n} |x_i - \mu|^2\right)}{n-1} \tag{3.2}$$

$$\sigma = \sqrt{\sigma^2} \tag{3.3}$$

As a basis to compare the homogeneity of a mixture the intensity of segregation, a dimensionless number, is employed in this work. Intensity of segregation, which was originally developed by P. V. Danckwerts circa 1952, is calculated by dividing the compound percent variance by the two mean values of each component compound percent. The represented calculation of intensity of segregation, I, is shown in Equation 3.4. I reflects not on the relative amounts of [components] A or B nor the size of the clumps, but the extent to which the concentration in the clumps departs from the mean[12]. In other words, intensity of segregation depends on the dilution of the two constituents. When segregation is complete, the intensity of segregation will equal to one. As the intensity of segregation decreases, the homogeneity of the mixture increases. The dimensionless number also serves as a method to compare mixtures with different sample weight ratios.

$$I = \frac{\sigma^2}{\mu_1 \cdot \mu_2} \tag{3.4}$$

3.2 Visible Changes on SEM and EDS Images

As the homogeneity of the mixture increases, visible changes on the SEM and EDS images can also be seen. For poor mixtures, there are large agglomerate regions of single elements that are easily visible on both the SEM and EDS images. The images from mixtures of silica Aerosil® R974 and Aeroxide® titania P25 were used in order to see the changes in the contrast of the secondary electron images.

An example of a poor mixture is presented in Figure 3.1. As mixture homogeneity increases, the visible agglomerate regions decrease in size. These decreases in agglomerate sizes are shown in Figures 3.2 through 3.4. Figure 3.5 shows how a well-mixed sample appears. There are no visible agglomerates on either the SEM or EDS images appearing in Figure 3.5. These images do not mean that there is mixing on the primary particle level, but that mixing is below the detection level of the SEM and EDS. While the image can be magnified farther than 5000x, no new quantitative data can be obtained at a higher magnification because the resolution of detection does not change.

The SEM and EDS images of a mixture can be associated with a value of intensity of segregation for that mixture. Table 3 documents an observed relationship, applicable to this work, between intensity of segregation and agglomerate sizes. Intensity of segregation decreases with the decrease in agglomerate size. Additional SEM and EDS images for the silica R974 and titania P25 mixtures, along with the calculated values of intensity of segregation for the image, can be found in Appendix A.

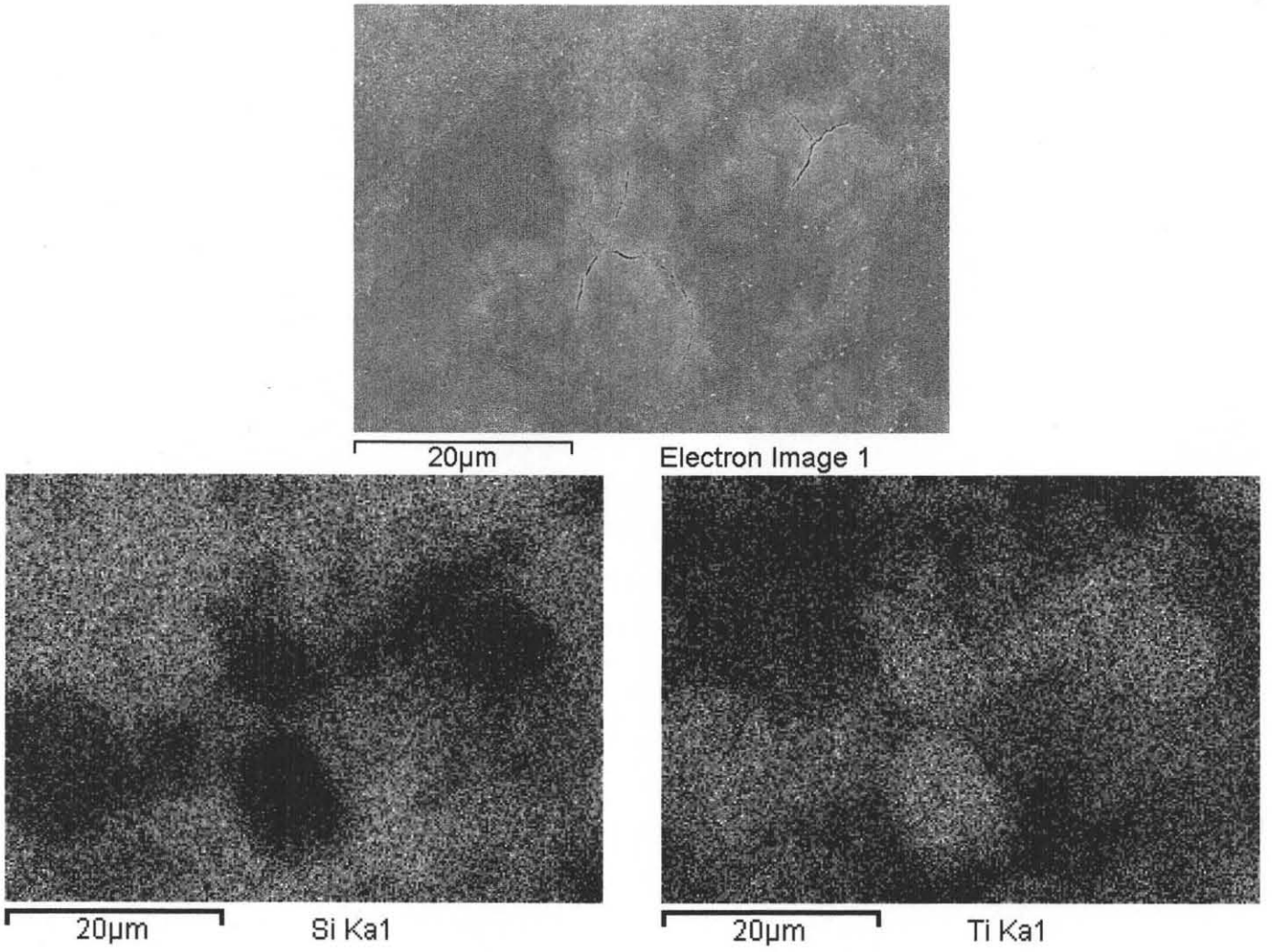

Figure 3.1 SEM and EDS images for poorly-mixed sample. Secondary electron image (top), silicon elemental mapping (left), titanium elemental mapping (right).

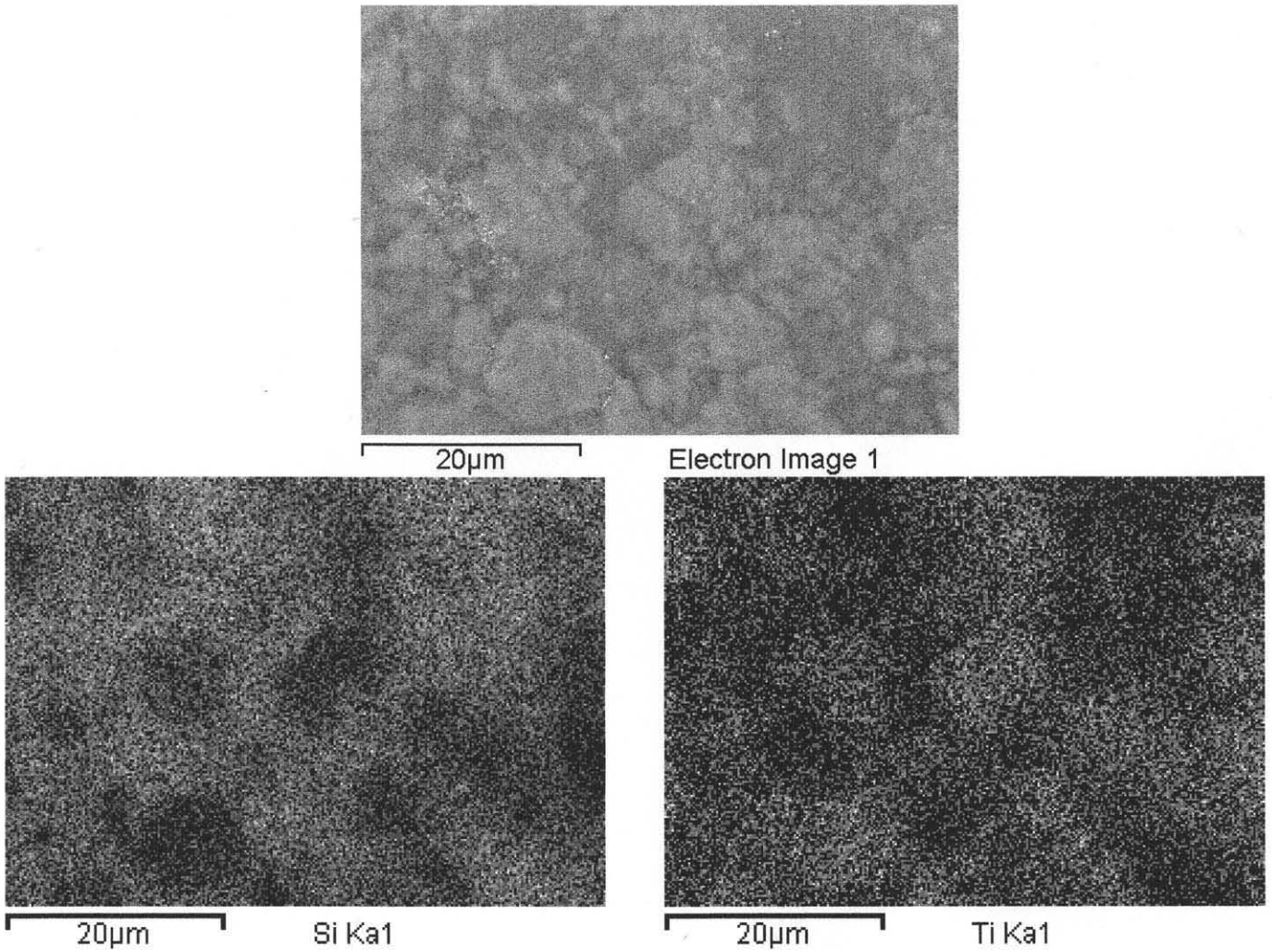

Figure 3.2 SEM and EDS Images. Secondary electron image (top), silicon elemental mapping (left), titanium elemental mapping (right).

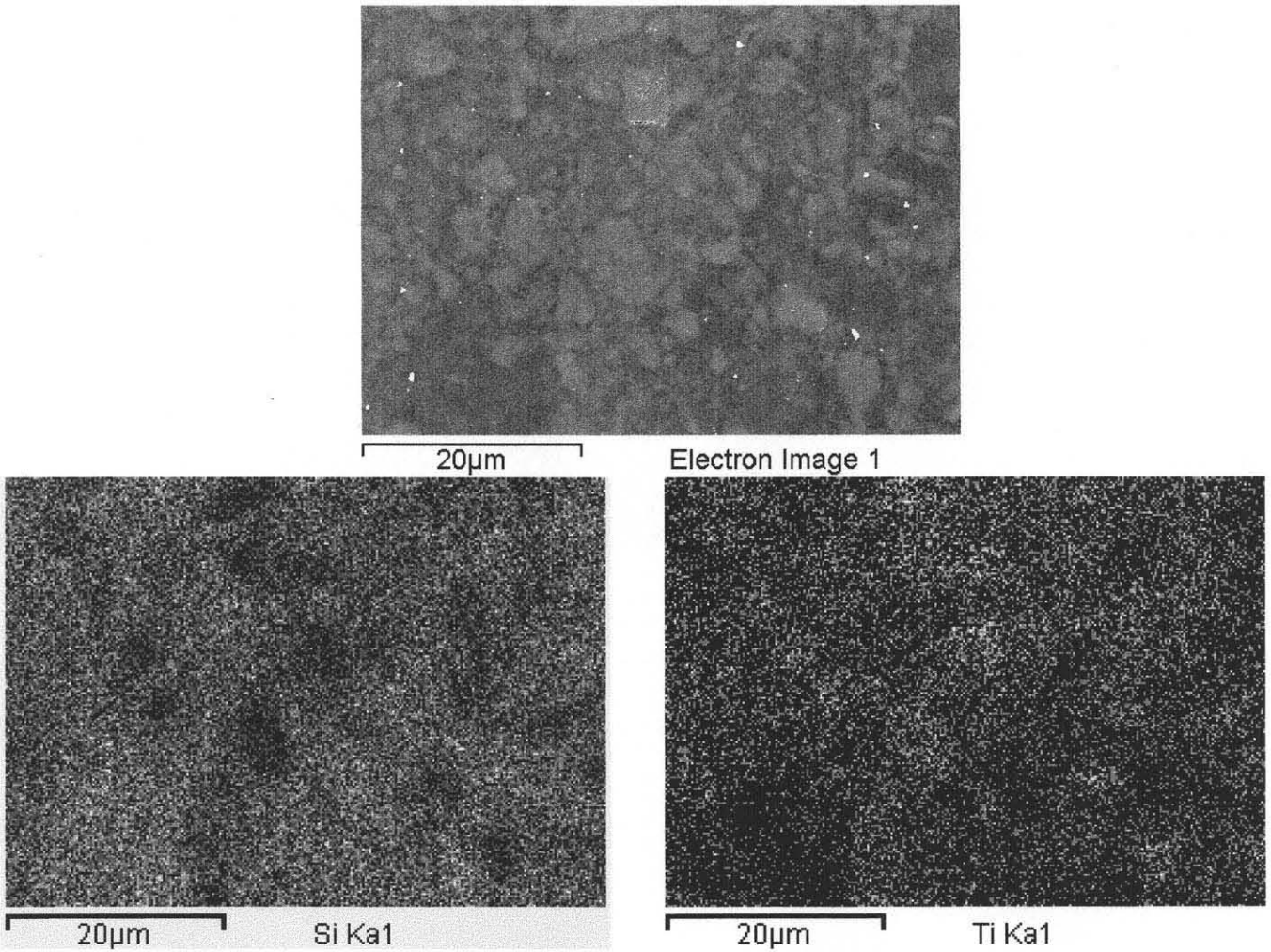

Figure 3.3 SEM and EDS Images. Secondary electron image (top), silicon elemental mapping (left), titanium elemental mapping (right).

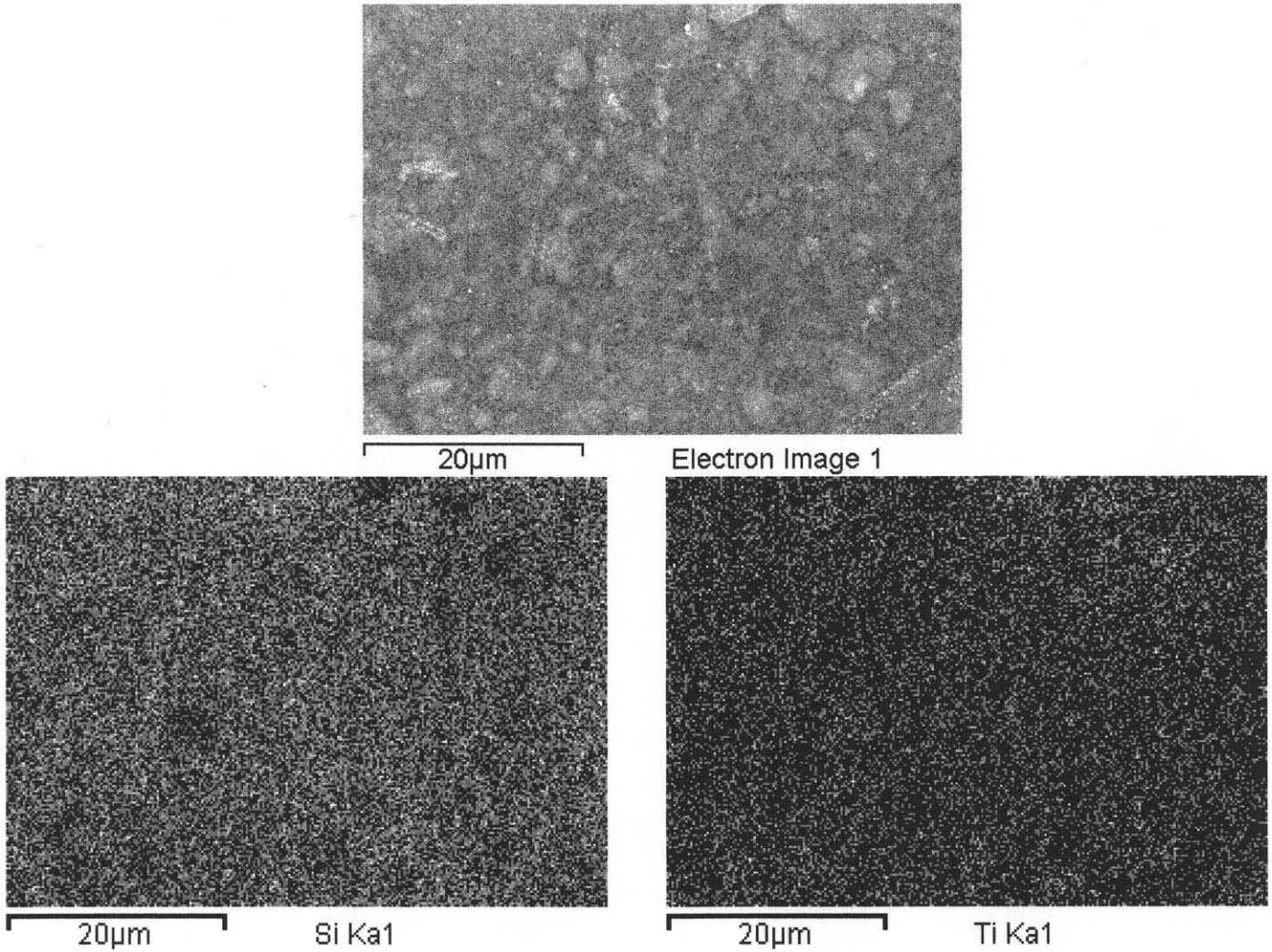

Figure 3.4 SEM and EDS Images. Secondary electron image (top), silicon elemental mapping (left), titanium elemental mapping (right).

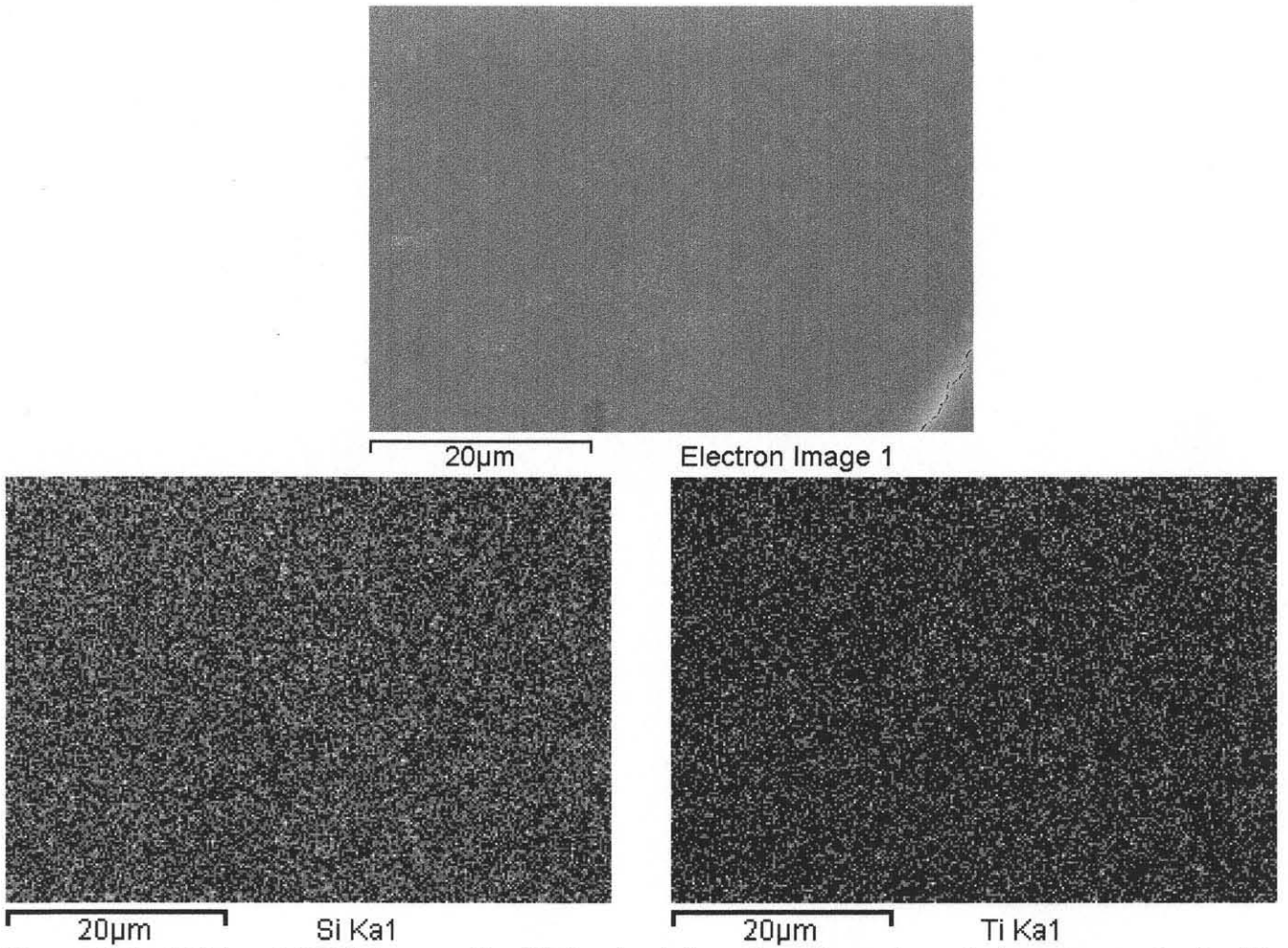

Figure 3.5 SEM and EDS Images for Well-mixed Sample. Secondary electron image (top), silicon elemental mapping (left), titanium elemental mapping (right).

Table 3 Comparison Between Intensity of Segregation and Agglomerate Size

Intensity of Segregation	Agglomerate Size SEM (microns)	Agglomerate Size EDS (microns)
0.4684	45	40
0.2741	20	30
0.1966	10	15
0.1264	15	15
0.0777	7	7
0.0128	< 5	5
0.0015	Below analysis level	

CHAPTER 4

Intensity of Segregation Results

In this chapter, details of the mixing results obtained through MAIM are presented. Results for the dependence of magnet-to-sample ratio, time, magnet size, and the second constituents of the mixture are presented in this chapter. Intensity of segregation is plotted versus magnet-to-sample ratio or time. The lower intensity of segregation indicates a better mixing quality.

4.1 Intensity of Segregation versus Magnet-to-sample Ratio

Magnet-to-sample ratio is the weight of the magnets to the total weight of the nanoparticles. One gram of each of the two constituents is measured out and combined with magnets. Previous research used magnet-to-sample weight ratios of 12:1, processed for 15 minutes[2], and 3:1, processed for 30 minutes[1], and had determined the mixture qualities to be poor. Experiments are carried out with magnet-to-sample weight ratios of 10:1, 5:1, 2:1, and 1:2; representing 20 grams of magnet for 2 grams of sample, 10 grams of magnet for 2 grams of sample, 4 grams of magnets for 2 grams of sample, and 1 gram of magnets for 2 grams of samples, respectively. Times of 30, 20, and 10 minutes are used to study the four magnet-to-sample ratios. The field strength was 15.5 milliteslas, the sample-to-sample weight ratio remained at 1:1, and a volume within the magnetic field of 80 milliliters was kept constant. The magnet size range was between 850 microns to 1400 microns. The results of the magnet-to-sample ratios appear in Figure 4.1. Figure 4.1 shows that for all three samples, increasing the magnet-per-sample ratio

lowers the intensity of segregation. With the increase of magnets, there is an increase in the number of magnet collisions with the agglomerates of nanoparticles, promoting deagglomeration and mixing.

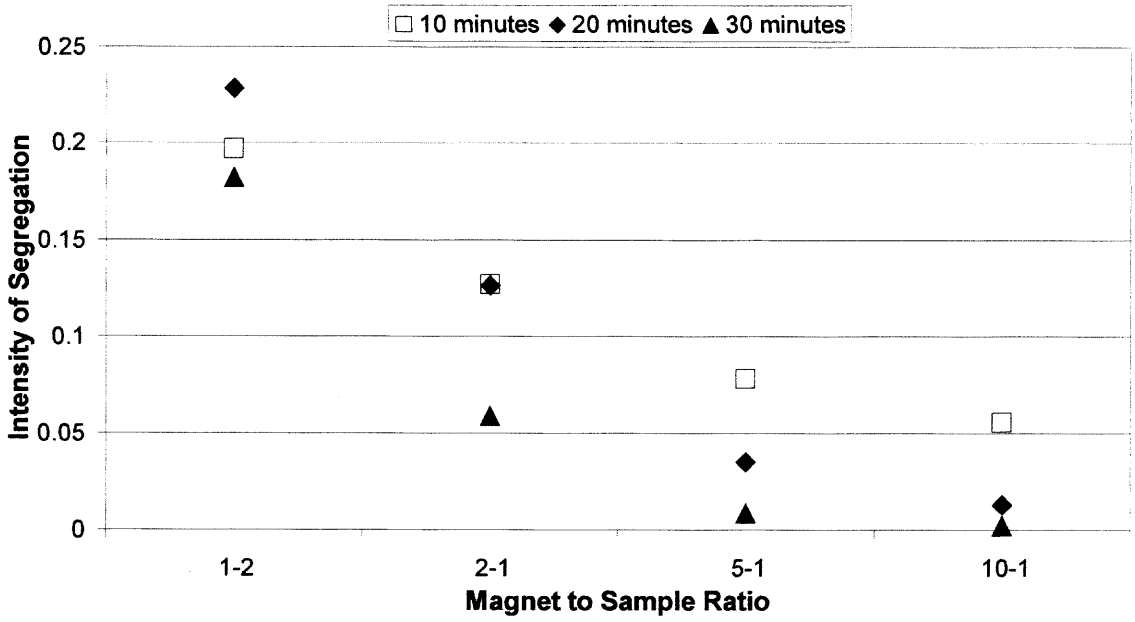

Figure 4.1 Intensity of segregation versus magnet-to-sample ratio.

4.2 Intensity of Segregation versus Time

The results from Figure 4.1 show that by increasing the magnets per sample there is a decrease in the intensity of segregation; however, the trends for time were not conclusive. MAIM processing time is studied closer to determine if there is a clear trend. Process times of 5, 40, 60, 90, and 120 minutes were added to the results of 10, 20, and 30 minutes. The field strength was 15.5 milliteslas, the sample-to-sample weight ratio remained at 1:1, and the volume of the container within the magnetic field was kept constant. The magnet size range was between 850 microns to 1400 microns. The results from studying the effect of processing time in MAIM mixing appear in Figure 4.2. It appears that as processing time increases, there is a decrease in the intensity of segregation, leading to a better mixture. The lines connecting the points on the figures are used for aesthetic clarity, and have no other significance. Of the two previous MAIM studies, the first study used a processing time of 30 minutes and magnet-to-sample ratios of 3:1[1], and the second study used a processing time of 15 minutes and a magnet to sample ratio of 13:1[2]. From Figure 4.2, it is apparent that better mixtures are obtained after longer processing times of at least 60 minutes.

After 120 minutes, it is not evident that the 1:2 magnet-to-sample ratio will reach the intensity of segregation of the higher magnet-to-sample ratios or level out at an equilibrium value of intensity of segregation. To determine if the 1:2 magnet-to-sample ratio would achieve intensity of segregations similar to the higher magnet-to-sample ratios a longer process time is required.

A single experiment is performed with a magnet-to-sample ratio of 1:2 and a processing time of 570 minutes. Figure 4.3 includes the new data point, which shows that with a long enough processing time, even a 1:2 magnet-to-sample ratio can produce a well-mixed sample, similar to higher magnet-to-sample ratios. As with the magnet-to-sample ratio, when there is an increase in the processing time, there are more magnet interactions with the agglomerates of nanoparticles promoting deagglomeration and mixing.

During longer processing times with high magnet-to-sample ratios, such as.10:1, there is a caking effect. This can be explained due to the weight of the magnetic particles, and the amount of deagglomeration that is taking place, the powder tends to accumulate at the bottom of the container. The caking effect is the primary reason the 10:1 magnet to sample ratio was not studied further in the case study of magnet size.

4.3 Intensity of Segregation versus Magnet Size

The magnet size was also studied. The field strength was 15.5 milliteslas, the sample-to-sample weight ratio remained at 1:1, and the volume of the container within the magnetic field was kept constant. Three magnet size ranges were used representing large, medium, and small. The large magnets have a size range from 2360 microns to 1700 microns. The medium magnets, which were used in the other studies, have a size range from 1400 microns to 850 microns. The small magnets were in the range of 1000 microns to 600 microns. The focus of this study was carried out with magnet-to-sample ratios of 1:2, 2:1, and 5:1.

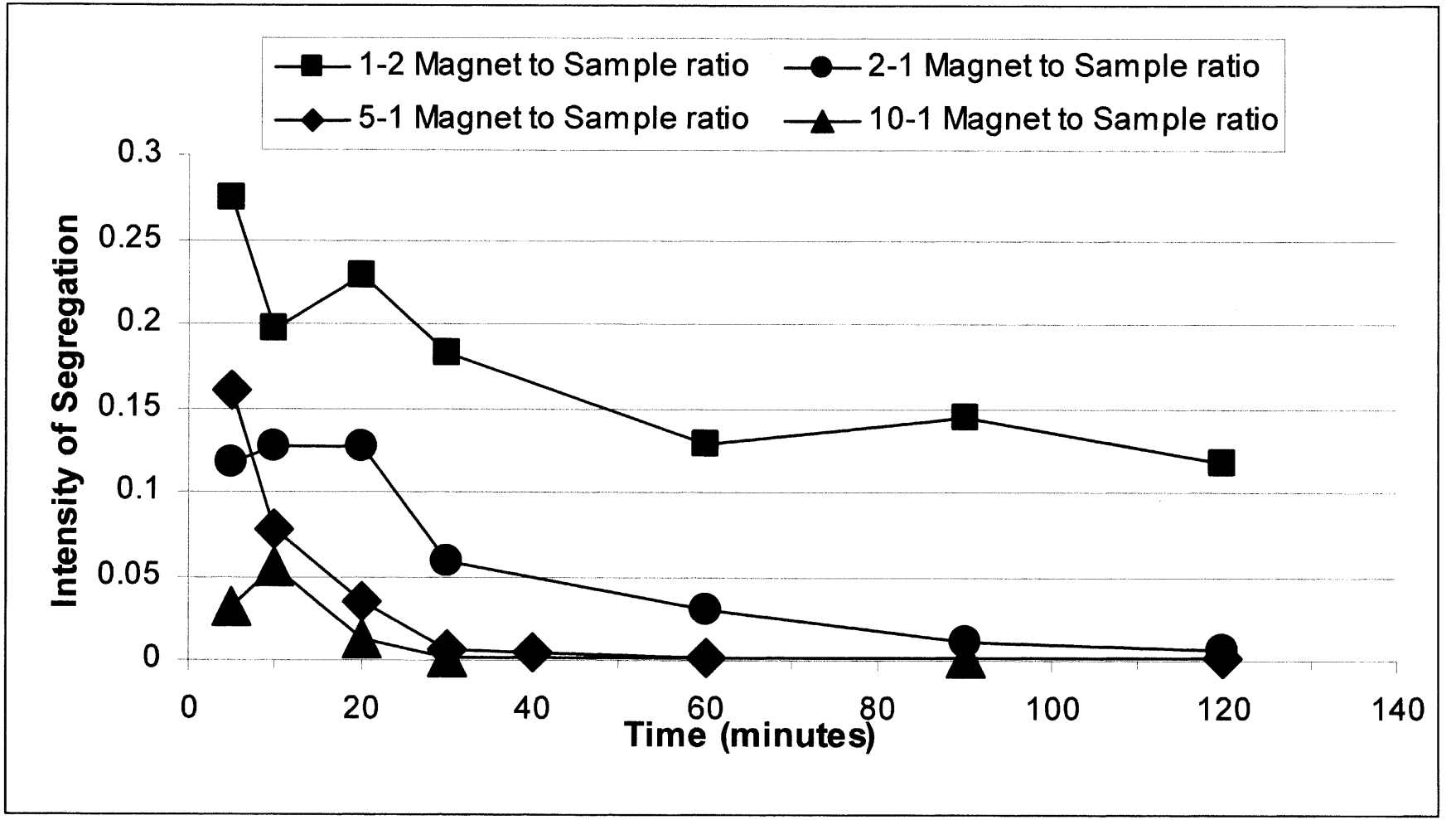

Figure 4.2 Intensity of segregation versus time.

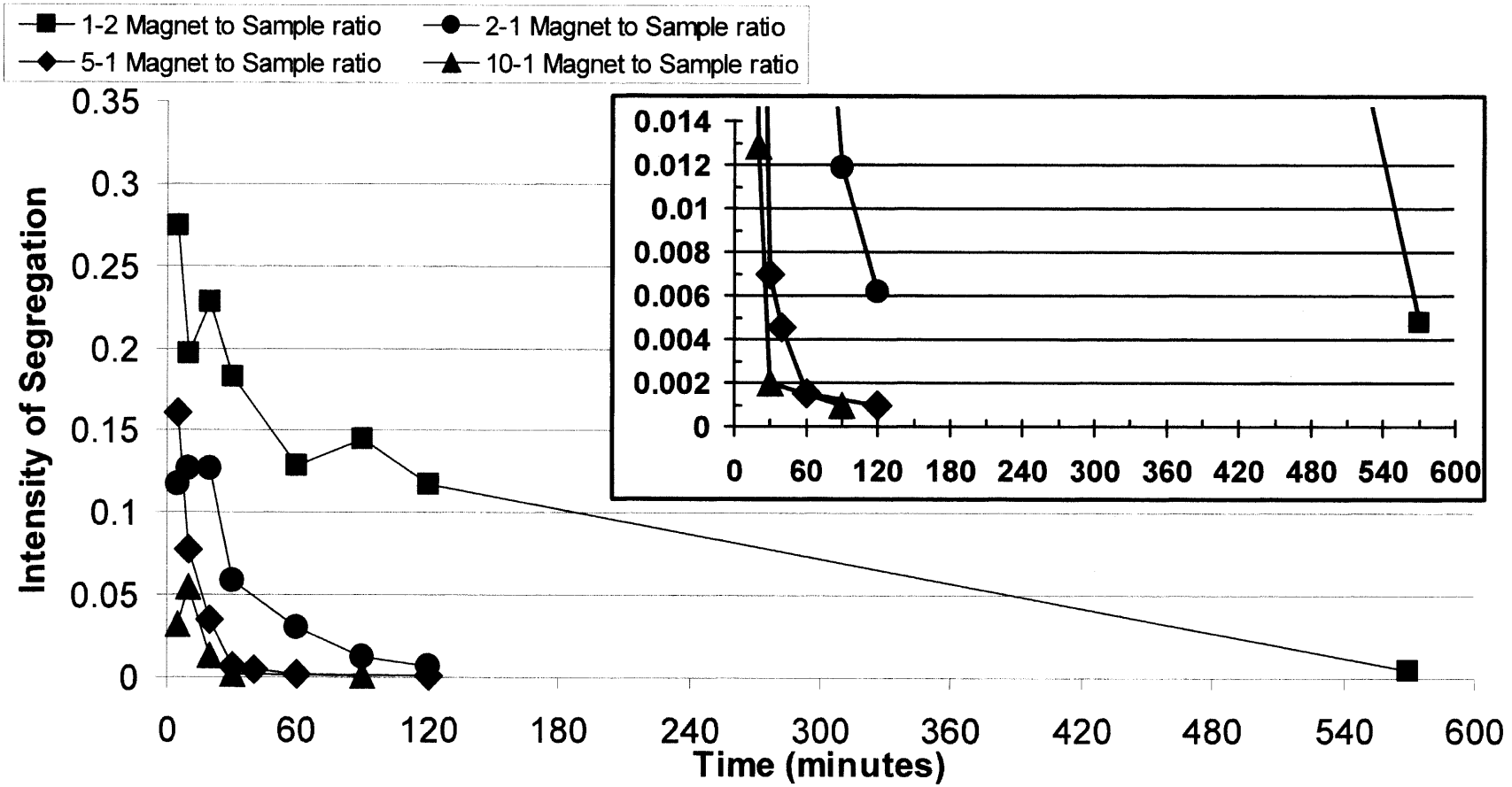

Figure 4.3 Intensity of segregation versus time.

Figure 4.4 contains the 1:2 magnets to sample ratio results. The overall mixture quality is poor for all mixtures, but the data points show a trend of decreasing intensity of segregation with the decrease in the size of the magnets. Figure 4.5 contains the 2:1 magnets to sample ratio results. Figure 4.6 contains the 5:1 magnets to sample ratio results. The 1:2, 2:1, and 5:1 magnet-to-sample ratio figures agree. When using smaller magnets, at the same processing time, a lower intensity of segregation is obtained. When weights of the same magnets are kept at a constant between the different magnet sizes, there are more magnets present for the smaller scale of magnets. The results from the magnet size matches the results obtained from magnet-to-sample ratio and time. When there are more magnets present, there are more magnet collisions, creating a better mixture with lower intensity of segregations. To determine the true effect of magnet size on the intensity of segregation, a future study should focus on keeping the number of magnets the same while changing the magnet size. While this approach could be potentially time consuming, since the magnets are only about one millimeter, nevertheless, it can be done.

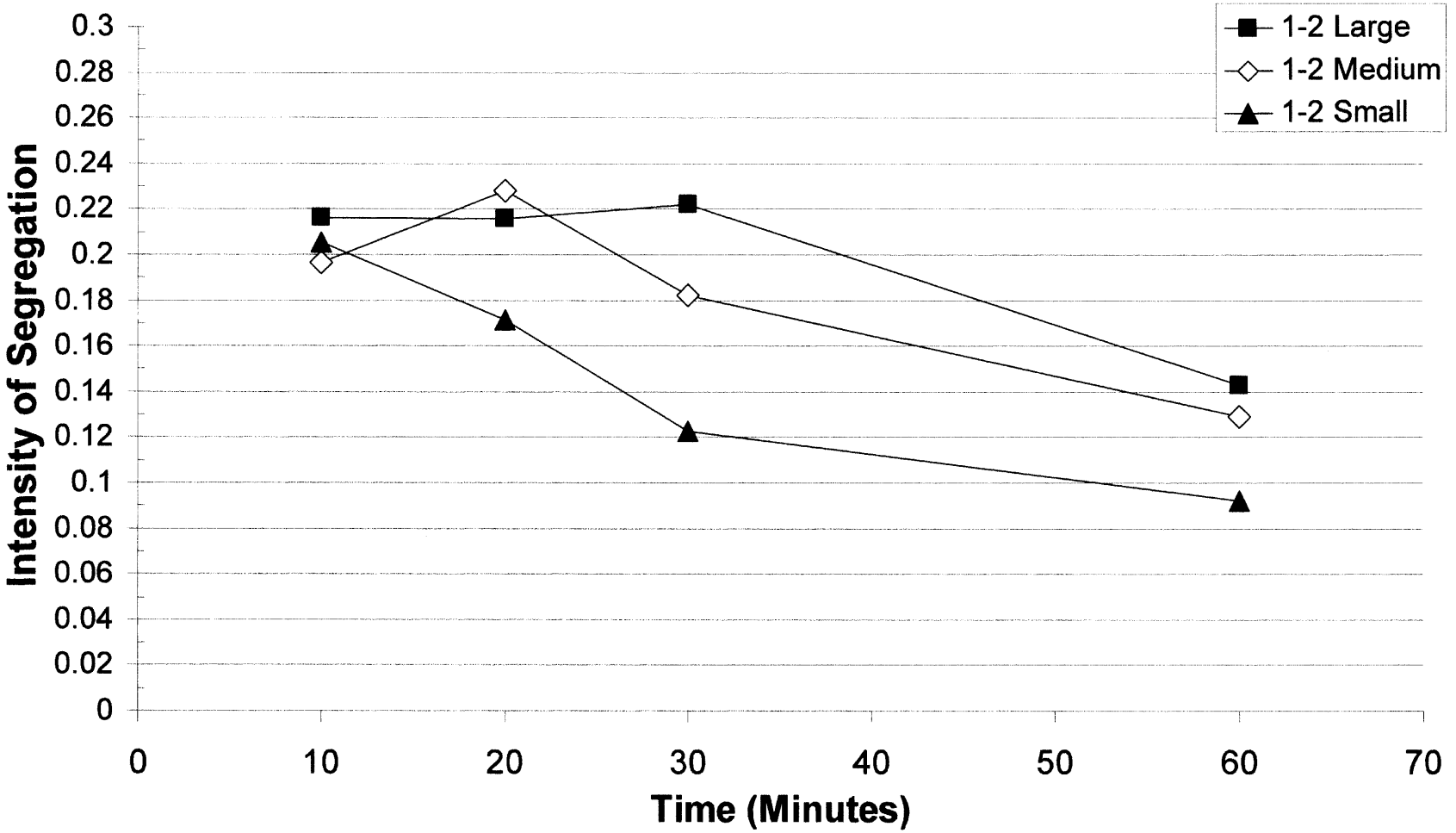

Figure 4.4 Intensity of segregation versus magnet size for a magnet-to-sample ratio of 1 to 2.

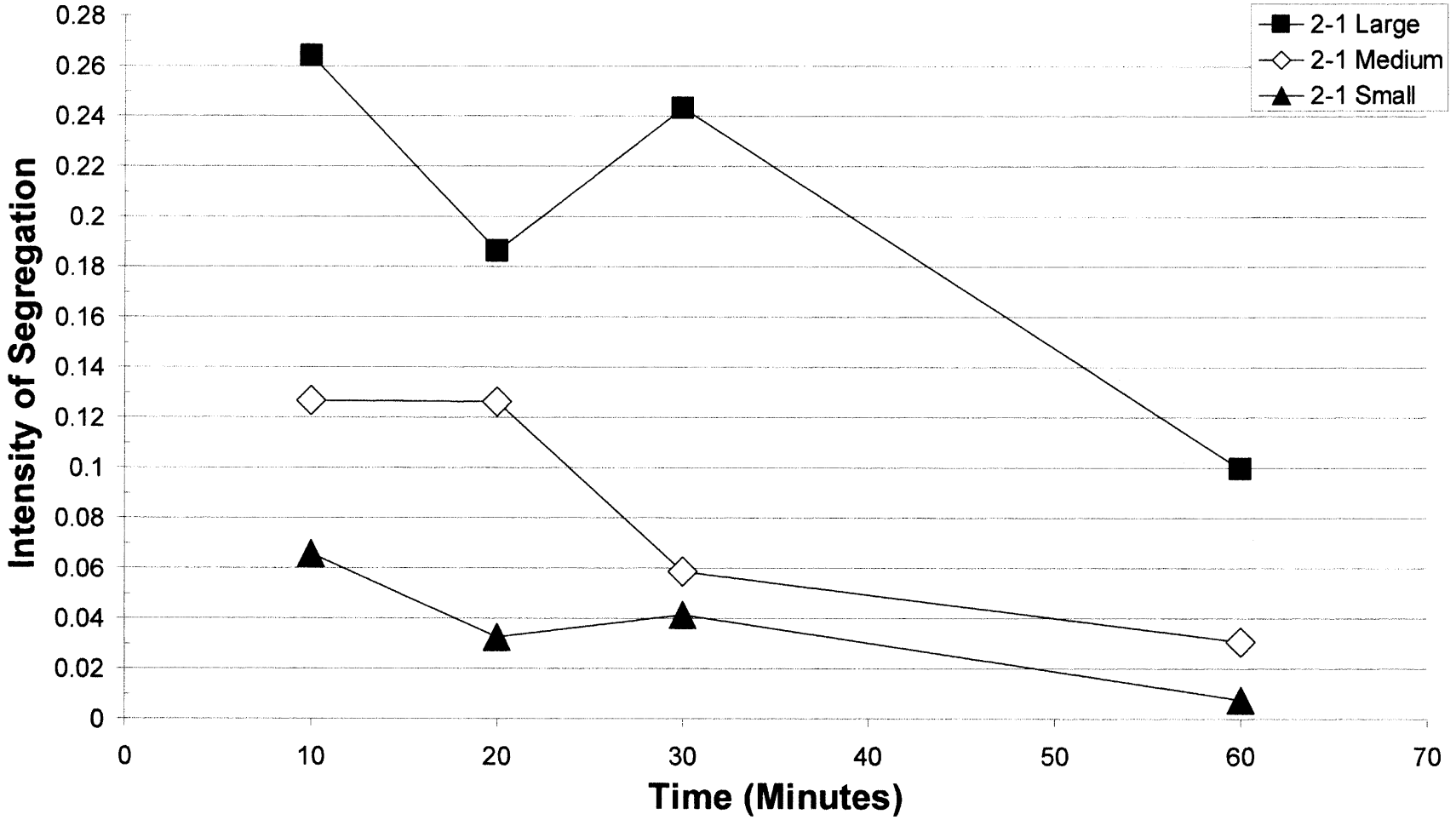

Figure 4.5 Intensity of segregation versus magnet size for a magnet-to-sample ratio of 2 to 1.

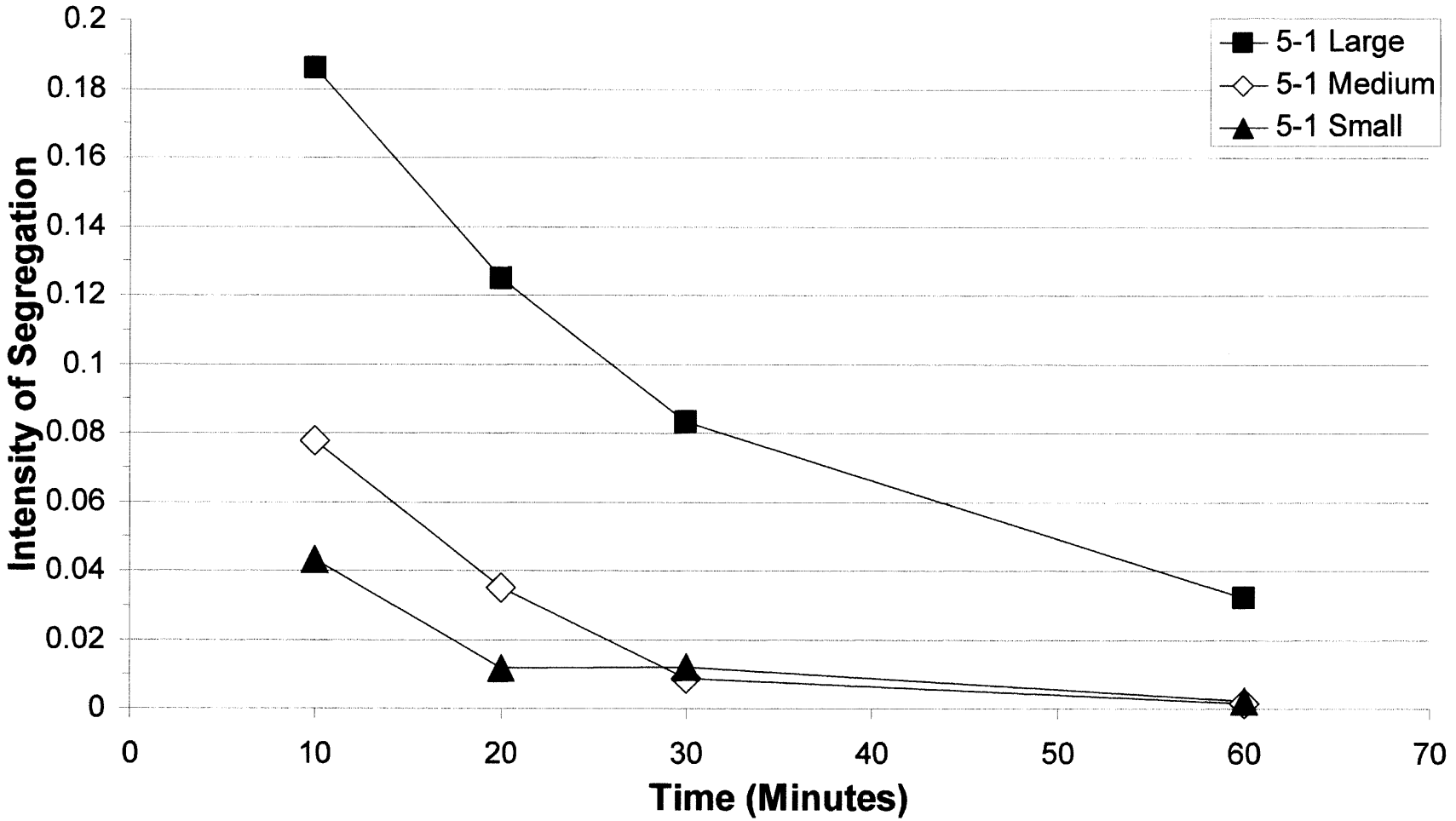

Figure 4.6 Intensity of segregation versus magnet size for a magnet-to-sample ratio of 5 to 1.

4.4 Intensity of Segregation versus Components

The last variable studied involves varying the second constituent of nanoparticle in the mixture, keeping the silica Aerosil® R974 constant, and switching between the Aeroxide® titania P25 and Aeroxide® alumina Alu C. The field strength was 15.5 milliteslas, the sample-to-sample weight ratio remained at 1:1, and the volume of the container within the magnetic field was kept constant. The magnet size range was between 850 microns to 1400 microns. Magnet-to-sample weight ratios of 10:1, 5:1, 2:1, and 1:2 were studied.

The resultant intensity of segregation data appears in Figure 4.7, with the silica-titania mixtures represented by the shaded points and the silica-alumina represented by the clear points. Similar trends are noticed between the different samples of the same magnet-to-sample weight ratio. In general, the alumina-silica mixtures have a lower intensity of segregation.

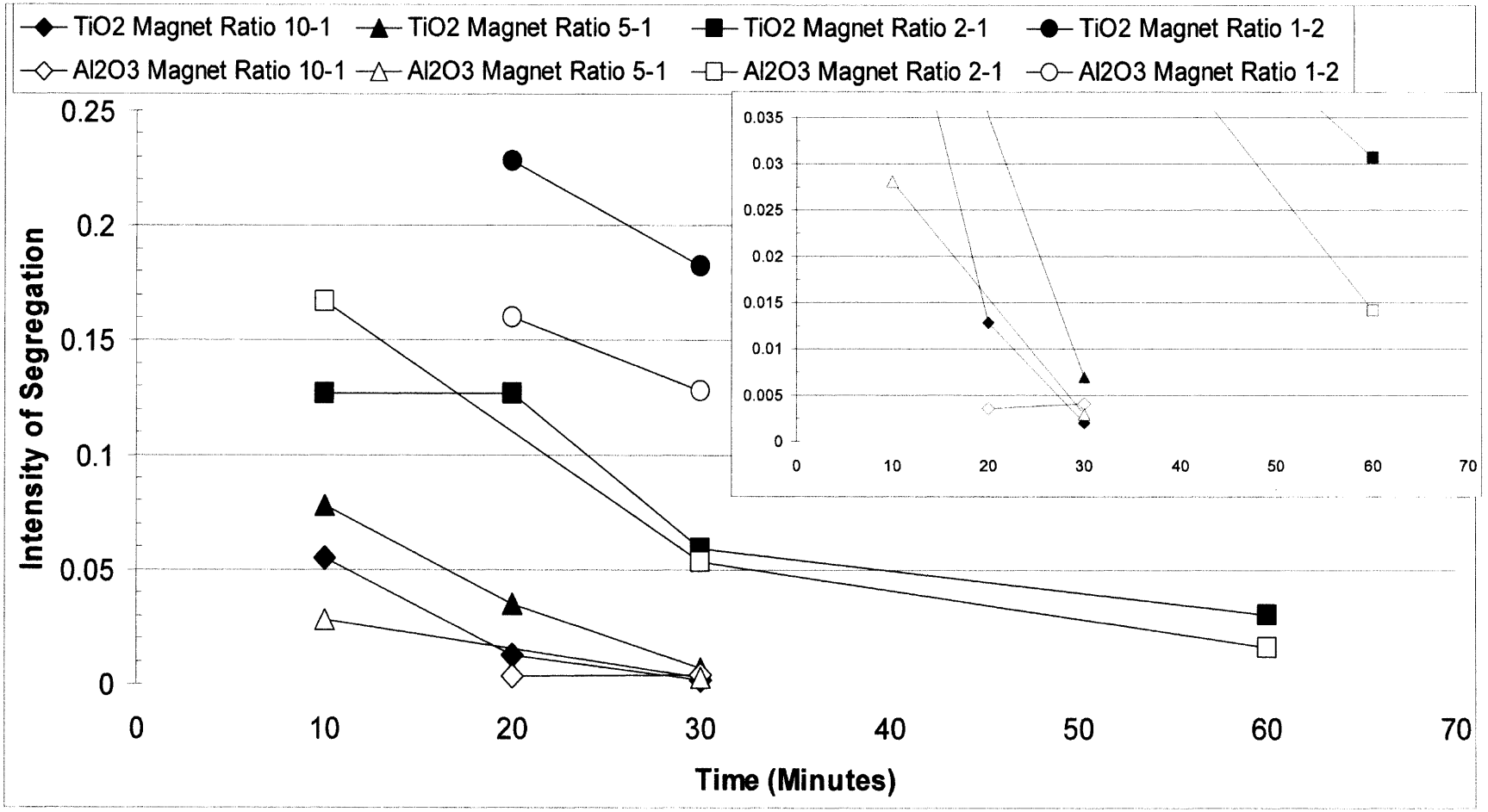

Figure 4.7 Intensity of segregation versus constituents.

4.5 Intensity of Segregation versus Mixing Technique

To determine how MAIM compares to other mixing techniques, results from five other techniques were used. The weight ratio of 1 to 1 for each of the nanoparticles remained a constant for each technique. The additional mixing techniques are fluidize bed mixing, supercritical stirring, assisted fluidize bed mixing, rapid expansion of supercritical solutions (RESS), high-pressure rapid expansion (HPRE), and supercritical sonication. These methods are environmentally benign using air, nitrogen, or carbon dioxide as a medium.

For fluidized bed mixings, the nanoparticles are placed in a column and nitrogen flow is introduced from the bottom. The gas flow expands the bed height and creates a fluidized state. In order to improve the quality of fluidization of nanoparticles and nanoagglomerates in a gas fluidized bed, a variety of external force fields such as vertical sinusoidal vibration, rotation (in a rotating fluidized bed), applying an oscillating magnetic field to excite magnetic particles placed on the distributor of the fluidized bed, applying sound waves at relatively low frequency generated by a loudspeaker, or adding a secondary flow in the form of a jet have been used. These external force fields act to reduce the minimum fluidization velocity, eliminate plug formation and channeling, and achieve a smoother, more homogeneous, liquid-like fluidization. This research studied both unassisted fluidization and assisted fluidization using a secondary flow in the form of a jet to mix two species of nanoparticles to compare with MAIM and other mixing methods. The secondary flow from the jet creates shearing forces that breakdown the agglomerates of nanoparticles and improves both fluidization quality and mixing.

For RESS and HPRE mixing, the samples are charged into high-pressure vessel and the pressure is increased to either a supercritical or a high-pressure state. Slight agitation is created with stirring blades. The contents of the vessel are released through micron-sized nozzle. As the agglomerates of nanoparticles pass through the nozzle, a type of explosion occurs that breaks up the agglomerates and promotes mixing between the nanoparticles. Only the best point from RESS and HPRE is shown on this thesis. Supercritical stirring is similar to RESS, but after the pressure is increased, supercritical stirring relies only on the shear forces created by the mixing blades and not the rapid expansion through a nozzle.

Sonication is run in a high-pressure vessel in a medium of supercritical carbon dioxide. A sonication horn creates high-energy sonic waves to break up the agglomerates and promote mixing. Sonication mixing is carried out by Ganesh Sanganwar and Dr. Ram Gutpa at Auburn University.

Fluidized bed, assisted fluidized bed, RESS, and sonication used nanoparticles of alumina and silica R972, while titania and silica R974 nanoparticles were obtained from supercritical stirring, MAIM, and sonication mixing. The primary particle sizes of silica Aerosil® R974, alumina Aeroxide® Alu C, silica Aerosil® R972, and titania Aeroxide® P25 are 12, 13, 16, and 21 nanometers, respectively.

The best mixing results, for each of these methods, are presented in Figure 4.8. The intensity of segregation obtained from MAIM is significantly lower than fluidized bed, supercritical stirring, assisted fluidized bed, and RESS. MAIM showed comparable results to sonication mixtures of silica R974 and titania, but sonication with silica R972 and alumina Alu C did provide the best mixing. MAIM produced the best results of any

dry mixing technique. The numerical values of the intensity of segregation for each of the methods are presented in Table 4.5.

Table 4 Intensity of Segregation Versus Mixing Method

Mixing Technique	Nanoparticles	Intensity of Segregation ($x10^3$)
Fluidized Bed, 3hrs	R972-Alu C	317.36
Supercritical Stirring, 2000RPM, 30mins	R974-TiO_2 P25	97.92
Assisted Fluidized Bed, 90mins	R972- Alu C	9.24
RESS-HPRE, 1100psi	R972- Alu C	1.93
MAIM, 5:1, 2hrs	R974- TiO_2 P25	0.94
Sonication, 65%Amp	R974- TiO_2 P25	0.90
Sonication, 85%Amp	R972- Alu C	0.44

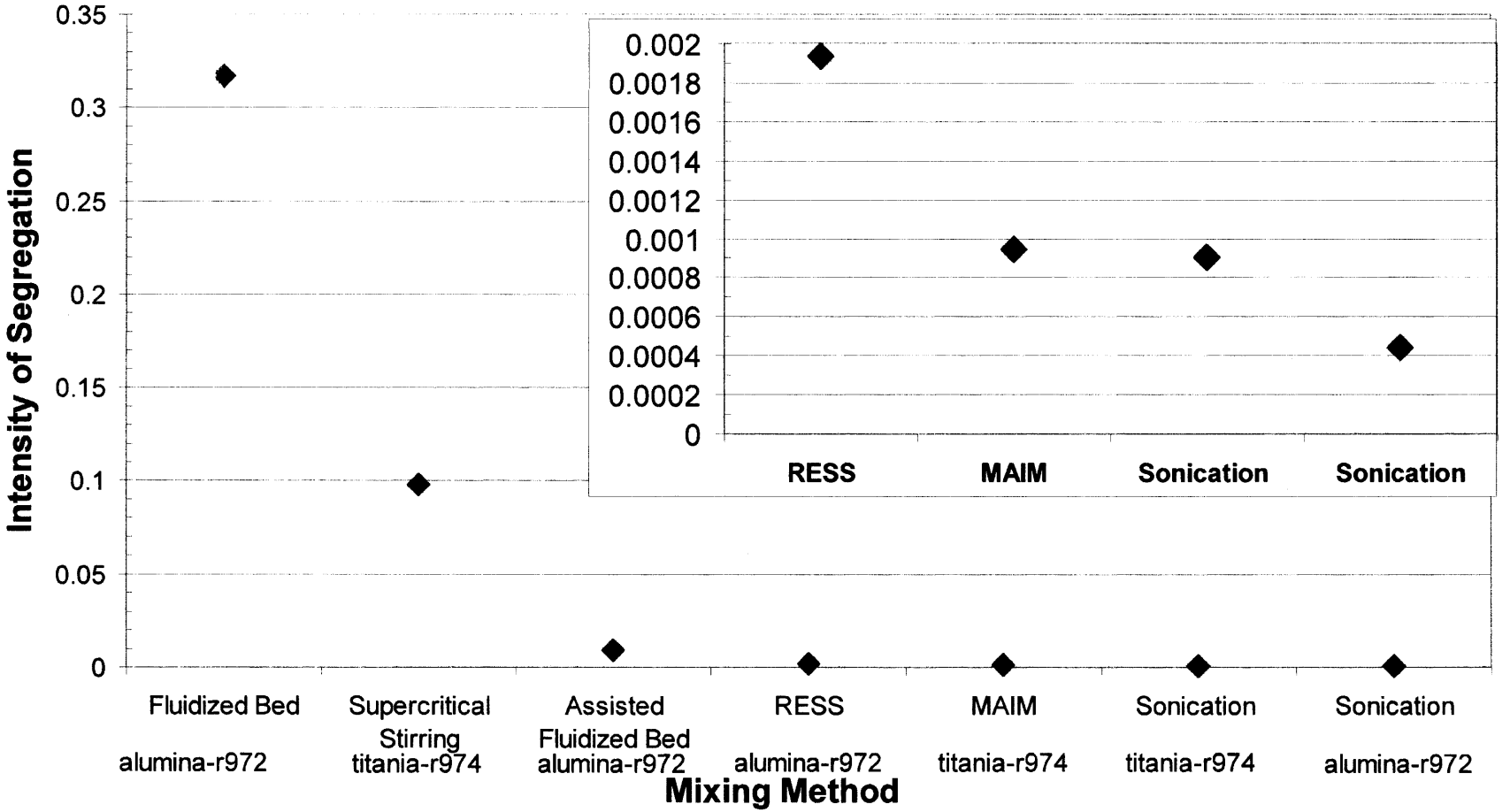

Figure 4.8 Intensity of segregation versus mixing technique.

CHAPTER 5

CONCLUSION

This thesis has focused on the dry mixing of nanoparticles by Magnetically Assisted Impaction Mixing. In order to mix nanoparticles on the nano-scale, there must be enough forces applied to break up the agglomerates. Alternate methods have been tried using shearing forces from mixing blades, the rapid expansion of supercritical solutions, and supercritical sonication. These methods usually require a medium of supercritical carbon dioxide. MAIM is an environmentally benign dry mixing technique that does not require further processing, such as conditioning or drying step.

As found in previous studies[13], the samples from the MAIM technique produced a mixture with significant deagglomeration and reduced mean particle size suggesting a better distribution. The deagglomeration is necessary for mixing nanoparticles because if the agglomerates are not broken down, mixing of nanoparticles will never reach a scale of a micron, let alone the nano-scale.

Mixtures consisted of 1:1 weight ratio of the two nanoparticles. In this study, the magnet-to-sample weight ratios of 10:1, 5:1, 2:1, or 1:2. The magnetic field strength is 15.5 milliteslas and the size of the container was not altered. For most of the studies, magnets in the size range of 1400 microns to 850 microns were used. Once the mixture is complete, the magnets are sieved, and two tablets are pressed for analysis.

Two sites of interest are randomly chosen and analysis is carried out with the use of a field emission electron microscope to image secondary electrons. Energy dispersive x-ray spectroscopy is also used to image elemental mappings, and to obtain compound

percentage data throughout the site of interest. A total of 400 points of compound percent data is processed and statistical analysis is calculated. The averages and variance are used to calculate the intensity of segregation[12], Intensity of segregation is a dimensionless number used as a method to determine the homogeneity of the mixture, with one equal to complete segregation.

Through the case studies carried out, MAIM can be optimized while avoiding potential slow downs. As magnet-to-sample ratios increases, the intensity of segregation decreases. However, if there are too many magnets, mixing will be hampered by caking on the bottom of the container. To remedy the caking effect, the container can be continually rotated or by using a stronger field strength to prevent the magnets from succumbing to the forces of gravity.

With the same magnet-to-sample ratios, processing time is studied from five minutes up to five-hundred-seventy minutes. As processing time increases, intensity of segregation decreases for all magnet-to-sample ratios. The resultant of the time case study shows that, giving a long enough processing time, all magnet-to-sample ratios, even a ratio of 1:2, can create a homogeneous mixture.

Magnet size ranges of 2360 to 1700 microns and 1000 to 600 microns are studied to compare to the data obtained from the magnet size range of 1400 to 850 microns. The weight ratios were kept constant for all magnet-to-sample ratios. While the true effect of magnet size was not determined, it is evident with all magnets in the studied size ranges, the amount of magnet interactions truly affect the homogeneity of the mixture.

Mixtures of silica Aerosil® R974 and alumina Aeroxide® Alu C were compared to original mixtures of Aerosil® R974 and Aeroxide® titania P25. While more studies

would be needed to determine the effect of the constituents, in this research mixtures of silica R974 and alumina Alu C created a more homogeneous mixture than silica R974 and titania P25, at the same conditions.

Mixture homogeneity improves as magnet-to-sample weight ratio increases, magnet size decreases, and processing time increases. In general, these three conditions increase the total number of magnet-magnet, magnet-wall, and magnet-powder collisions, thus mixing gets better as number of collisions increase.

The MAIM process is very effective in achieving mixing of nano-powders at sub-micron scale with results that are better than the typical RESS mixing results, and comparable to the sonication results. The MAIM process is simple, and a potentially scalable method that can be used on a wide variety of nano-materials

APPENDIX A

SAMPLING SITES

Figures A.1 to A.9 show secondary electron and x-ray mapping for different intensities of segregation.

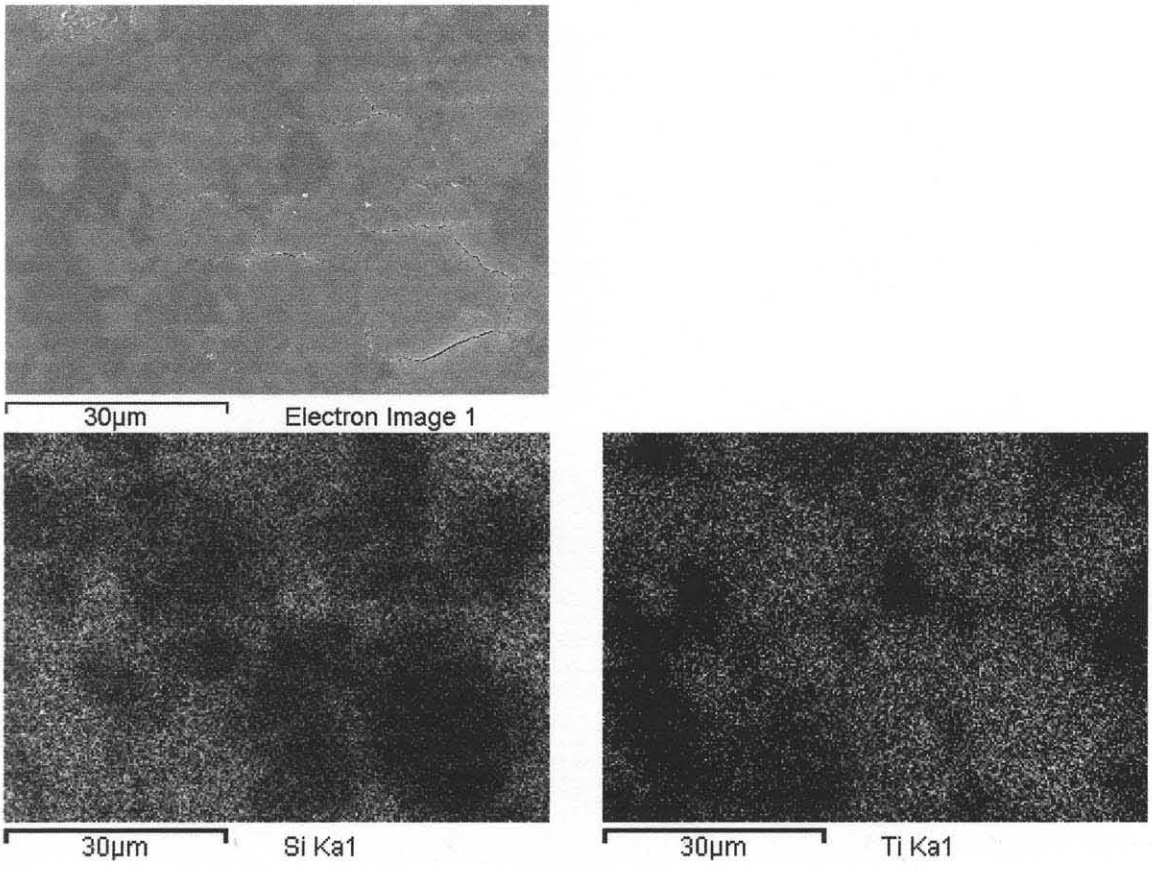

Figure A.1 SEM and EDS Images. For a sample with an intensity of segregation of 0.45. Secondary electron image (top), silicon elemental mapping (left), titanium elemental mapping (right).

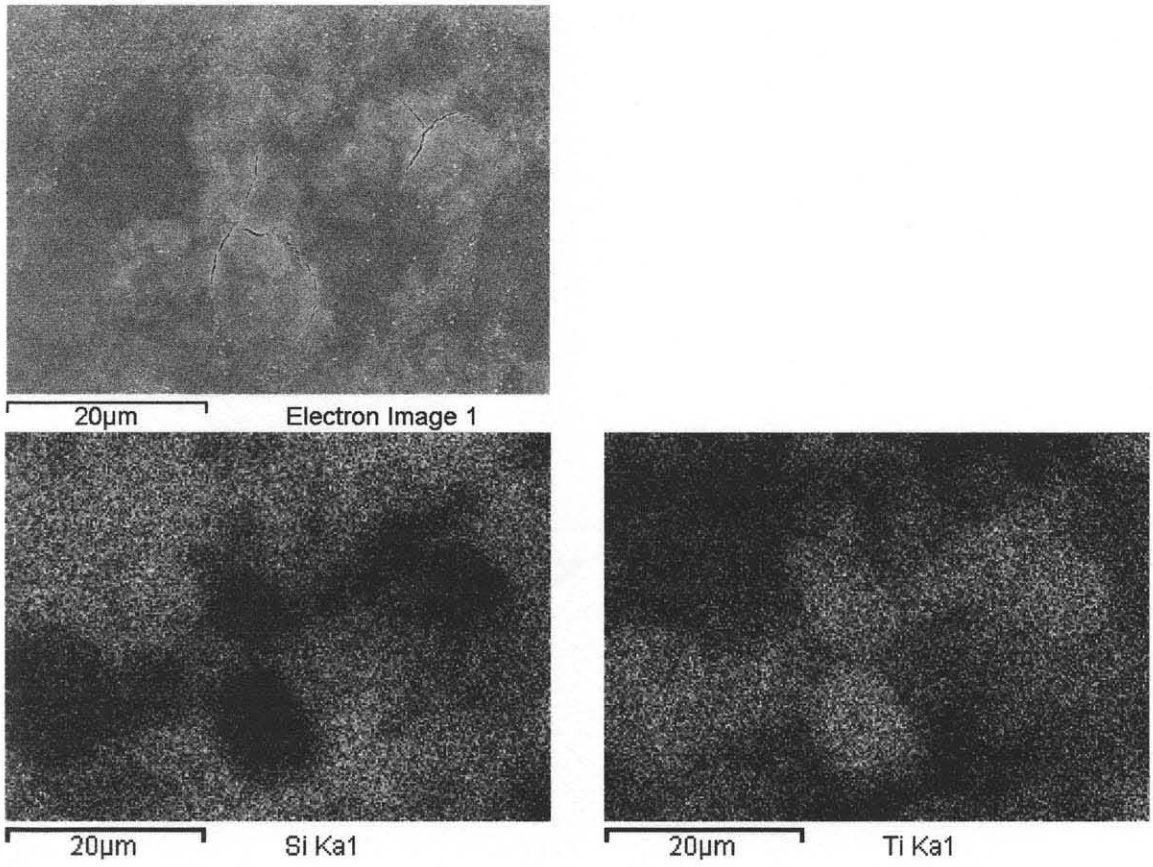

Figure A.2 SEM and EDS Images. For a sample with an intensity of segregation of 0.27. Secondary electron image (top), silicon elemental mapping (left), titanium elemental mapping (right).

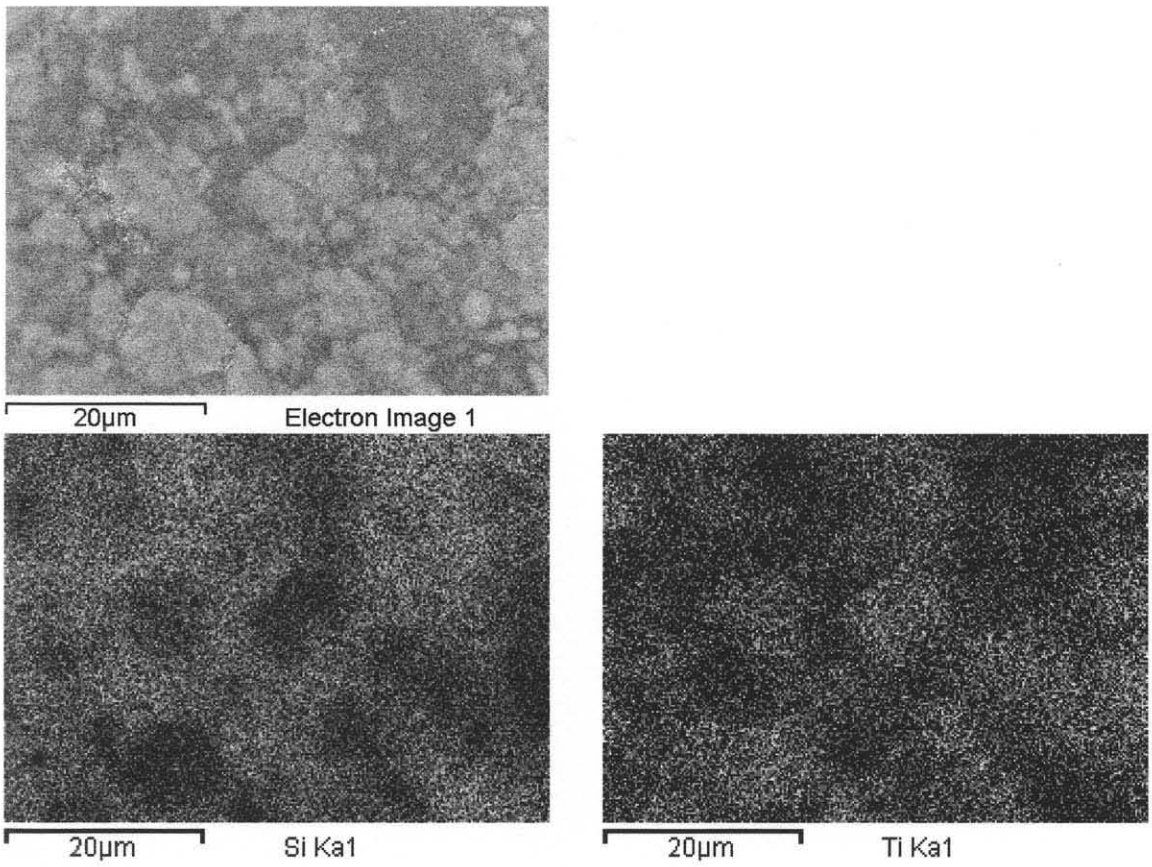

Figure A.3 SEM and EDS Images. For a sample with an intensity of segregation of 0.197. Secondary electron image (top), silicon elemental mapping (left), titanium elemental mapping (right).

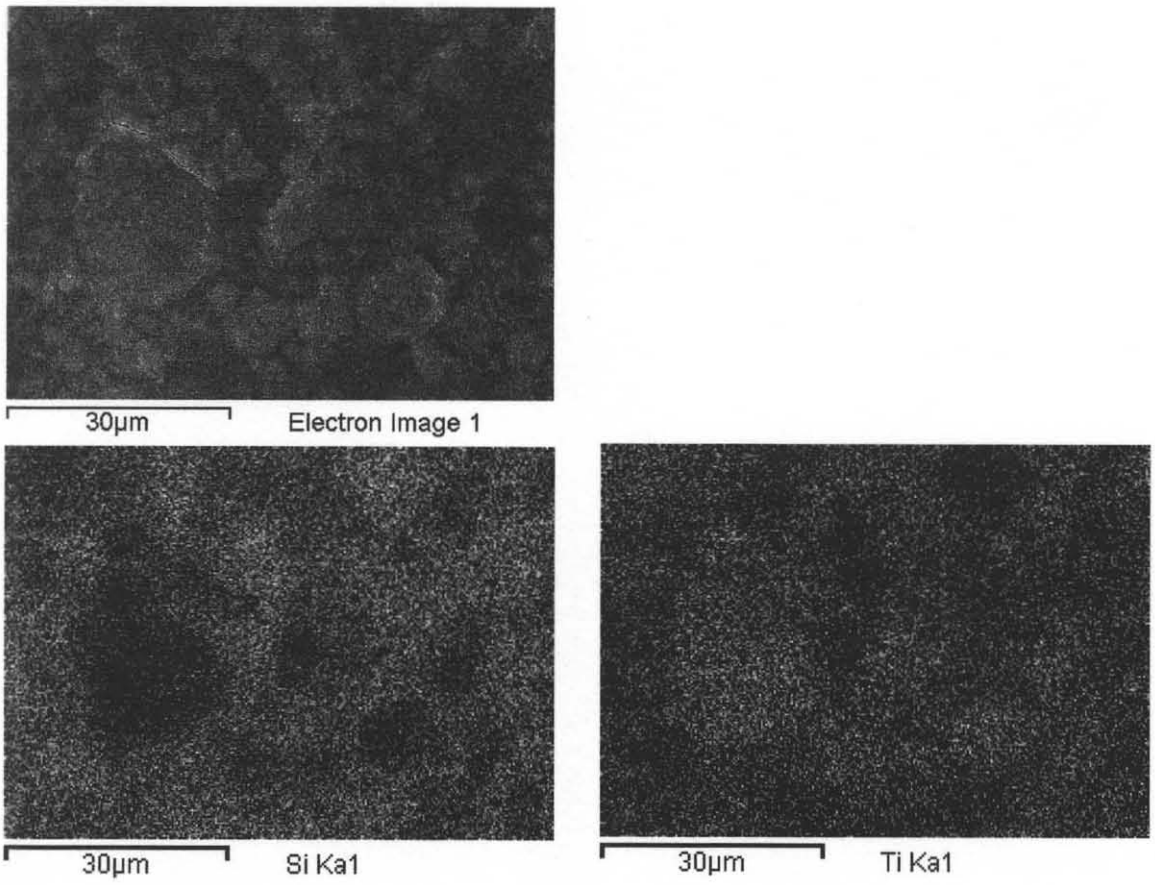

Figure A.4 SEM and EDS Images. For a sample with an intensity of segregation of 0.161. Secondary electron image (top), silicon elemental mapping (left), titanium elemental mapping (right).

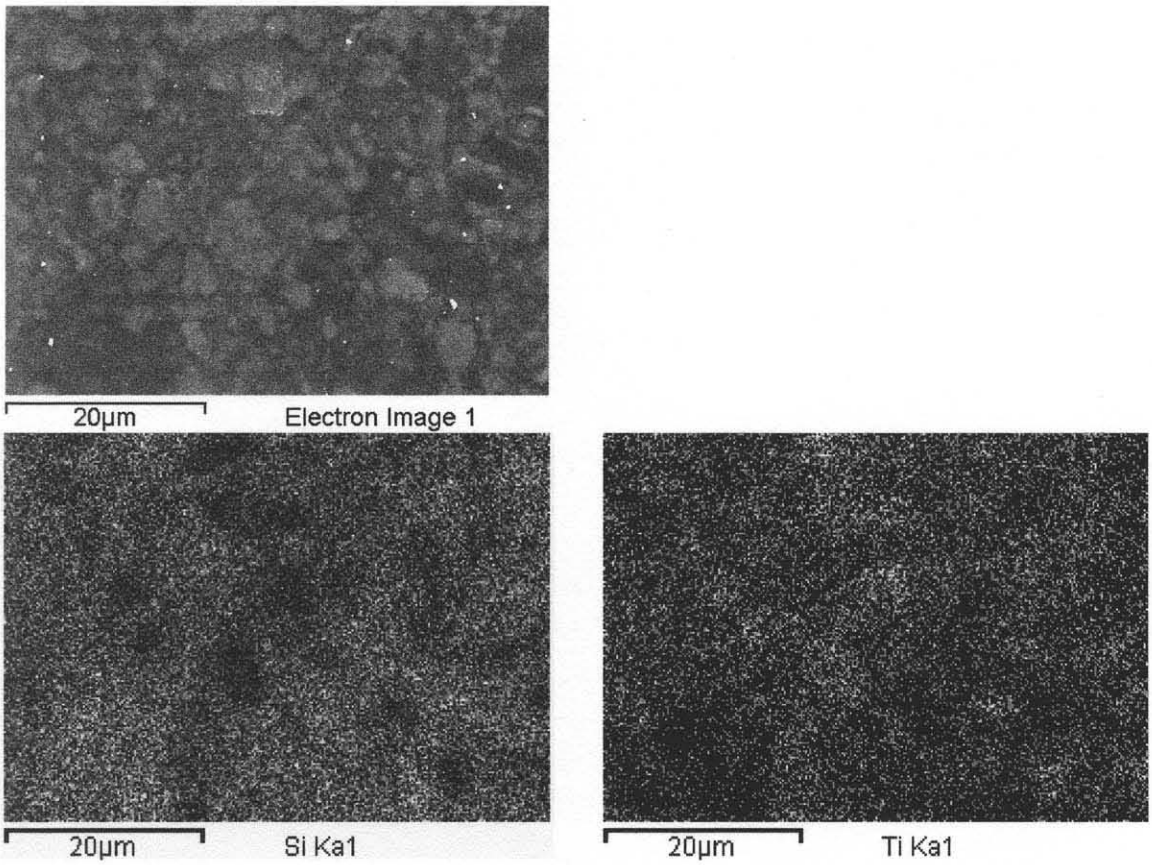

Figure A.5 SEM and EDS Images. For a sample with an intensity of segregation of 0.128. Secondary electron image (top), silicon elemental mapping (left), titanium elemental mapping (right).

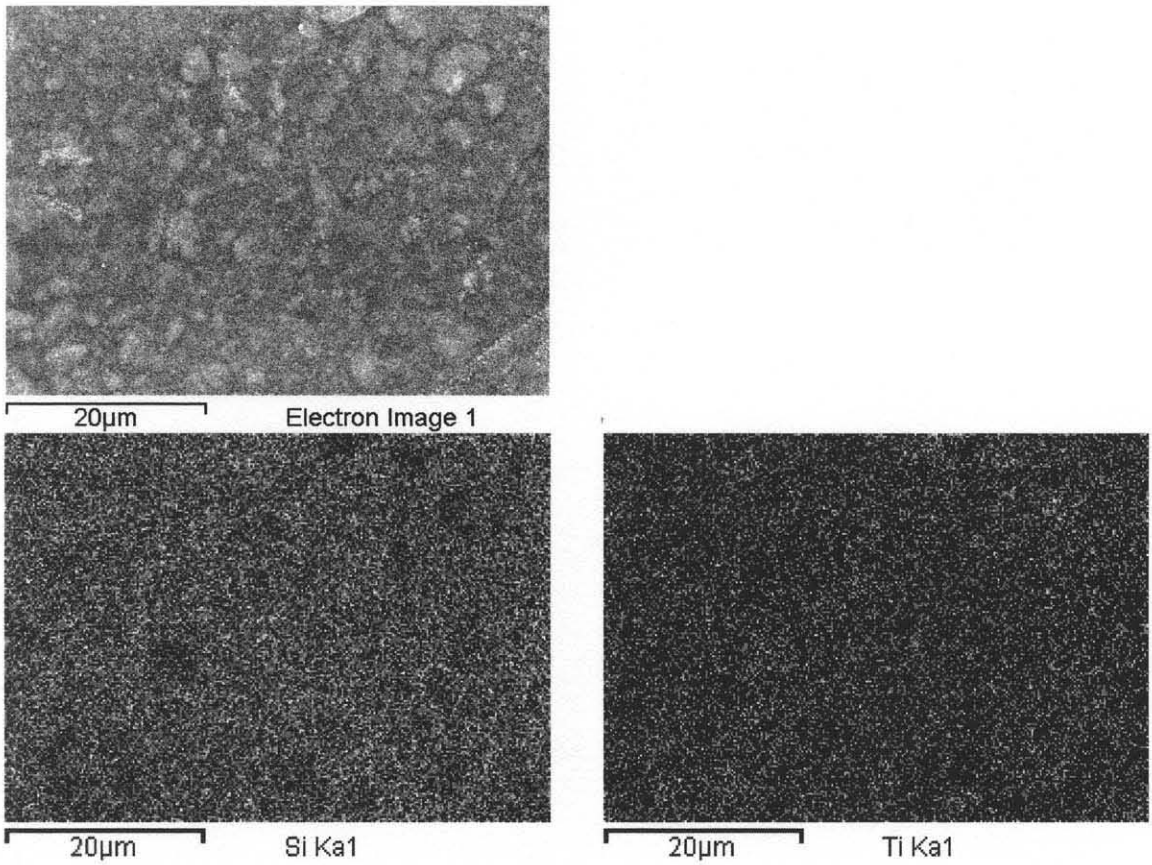

Figure A.6 SEM and EDS Images. For a sample with an intensity of segregation of 0.07. Secondary electron image (top), silicon elemental mapping (left), titanium elemental mapping (right).

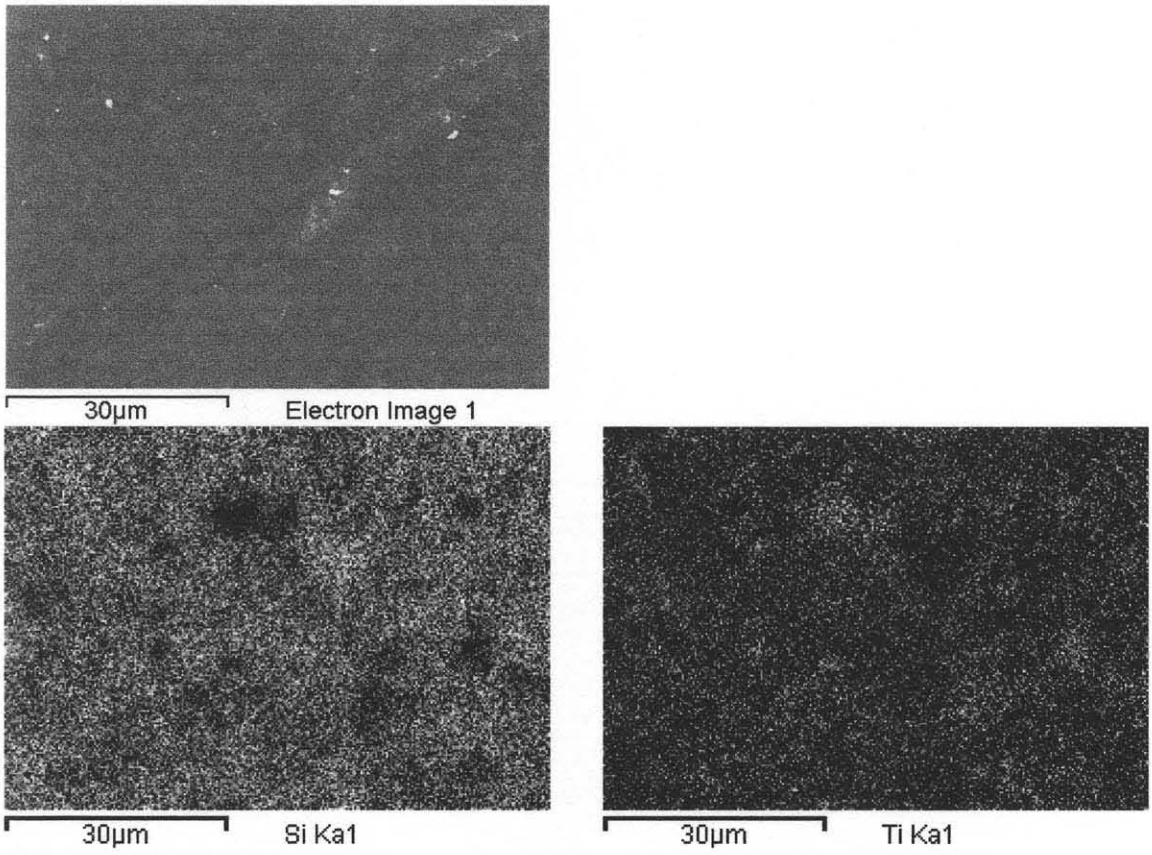

Figure A.7 SEM and EDS Images. For a sample with an intensity of segregation of 0.035. Secondary electron image (top), silicon elemental mapping (left), titanium elemental mapping (right).

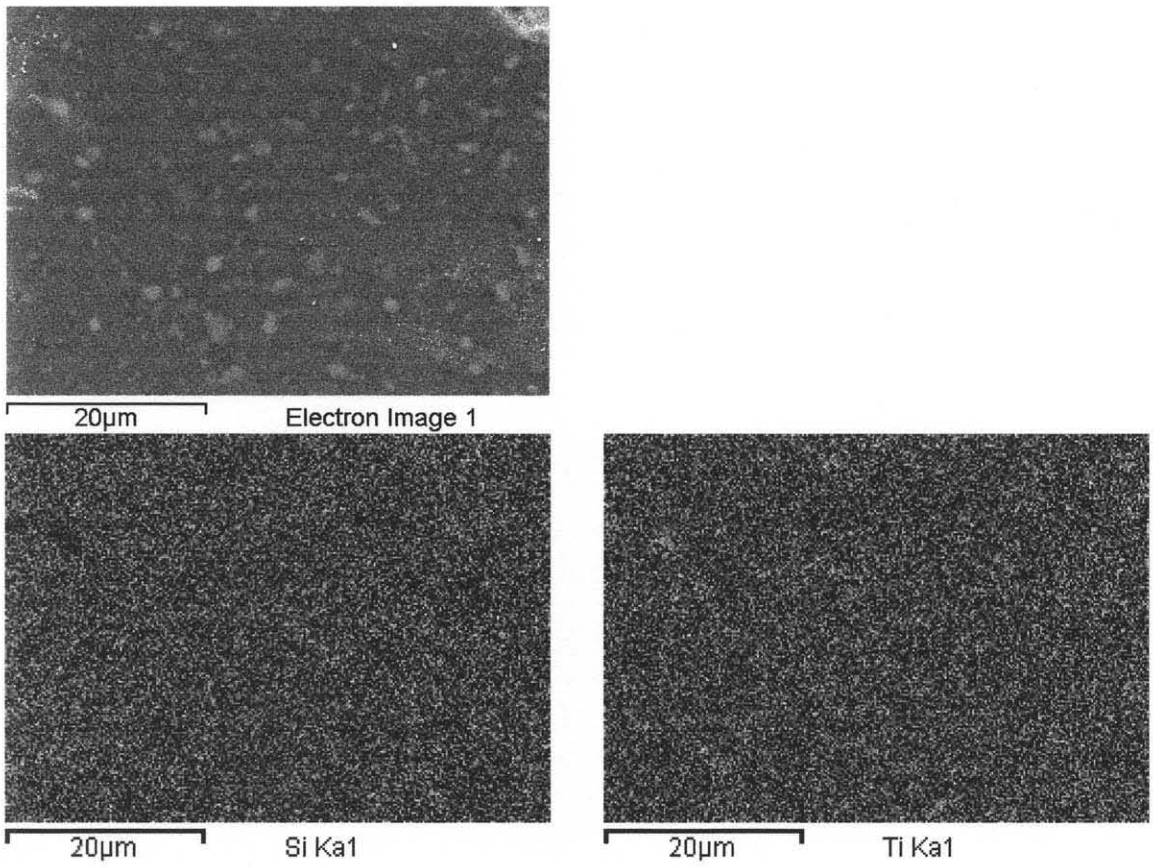

Figure A.8 SEM and EDS Images. For a sample with an intensity of segregation of 0.007. Secondary electron image (top), silicon elemental mapping (left), titanium elemental mapping (right).

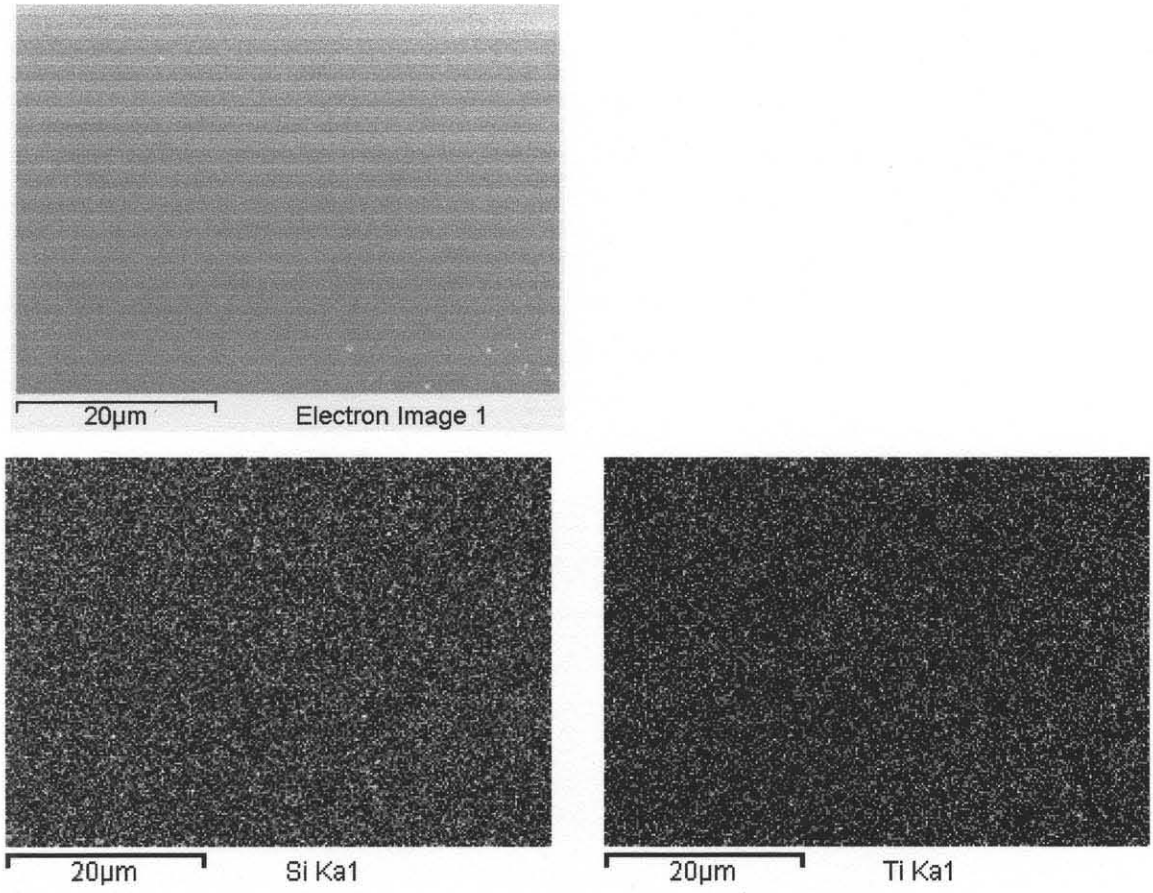

Figure A.9 SEM and EDS Images. For a sample with an intensity of segregation of 0.0009. Secondary electron image (top), silicon elemental mapping (left), titanium elemental mapping (right).

APPENDIX B

INTENSITY OF SEGREGATION DATA

Table B.1 contains all of the MAIM intensity of segregation data presented in this thesis.

Table B.1 Intensity of Segregation Data

Magnet-to-Sample Ratio	Time (min)	Magnet Size (μm)	Component A	Component B	Intensity of Segregation
1-2	10	1000-600	Silica R974	Titania P25	0.2055
1-2	20	1000-600	Silica R974	Titania P25	0.1716
1-2	30	1000-600	Silica R974	Titania P25	0.1228
1-2	60	1000-600	Silica R974	Titania P25	0.0919
1-2	5	1400-850	Silica R974	Titania P25	0.2741
1-2	10	1400-850	Silica R974	Titania P25	0.1966
1-2	20	1400-850	Silica R974	Titania P25	0.2281
1-2	30	1400-850	Silica R974	Titania P25	0.1822
1-2	60	1400-850	Silica R974	Titania P25	0.1290
1-2	90	1400-850	Silica R974	Titania P25	0.1452
1-2	120	1400-850	Silica R974	Titania P25	0.1171
1-2	570	1400-850	Silica R974	Titania P25	0.0048
1-2	20	2360-1700	Silica R974	Titania P25	0.2160
1-2	30	2360-1700	Silica R974	Titania P25	0.2221
1-2	60	2360-1700	Silica R974	Titania P25	0.1430
1-2	10	2360-1700	Silica R974	Titania P25	0.2162
2-1	10	1000-600	Silica R974	Titania P25	0.0657
2-1	20	1000-600	Silica R974	Titania P25	0.0324
2-1	30	1000-600	Silica R974	Titania P25	0.0415
2-1	60	1000-600	Silica R974	Titania P25	0.0077
2-1	5	1400-850	Silica R974	Titania P25	0.1170
2-1	10	1400-850	Silica R974	Titania P25	0.1268
2-1	20	1400-850	Silica R974	Titania P25	0.1264
2-1	30	1400-850	Silica R974	Titania P25	0.0589
2-1	60	1400-850	Silica R974	Titania P25	0.0307
2-1	90	1400-850	Silica R974	Titania P25	0.0119
2-1	120	1400-850	Silica R974	Titania P25	0.0062
2-1	10	2360-1700	Silica R974	Titania P25	0.2642
2-1	20	2360-1700	Silica R974	Titania P25	0.1862
2-1	30	2360-1700	Silica R974	Titania P25	0.2433
2-1	60	2360-1700	Silica R974	Titania P25	0.0994
5-1	10	1000-600	Silica R974	Titania P25	0.0433
5-1	20	1000-600	Silica R974	Titania P25	0.0118

5-1	30	1000-600	Silica R974	Titania P25	0.0121
5-1	60	1000-600	Silica R974	Titania P25	0.0022
5-1	20	1400-850	Silica R974	Titania P25	0.0351
5-1	30	1400-850	Silica R974	Titania P25	0.0069
5-1	40	1400-850	Silica R974	Titania P25	0.0045
5-1	60	1400-850	Silica R974	Titania P25	0.0015
5-1	120	1400-850	Silica R974	Titania P25	0.0009
5-1	5	1400-850	Silica R974	Titania P25	0.1610
5-1	10	1400-850	Silica R974	Titania P25	0.0777
5-1	20	2360-1700	Silica R974	Titania P25	0.1249
5-1	30	2360-1700	Silica R974	Titania P25	0.0834
5-1	60	2360-1700	Silica R974	Titania P25	0.0321
5-1	10	2360-1700	Silica R974	Titania P25	0.1862
10-1	5	1400-850	Silica R974	Titania P25	0.0318
10-1	10	1400-850	Silica R974	Titania P25	0.0552
10-1	20	1400-850	Silica R974	Titania P25	0.0128
10-1	30	1400-850	Silica R974	Titania P25	0.0020
10-1	90	1400-850	Silica R974	Titania P25	0.0010
1-2	20	1400-850	Silica R974	Alumina Alu C	0.1602
1-2	30	1400-850	Silica R974	Alumina Alu C	0.1281
2-1	10	1400-850	Silica R974	Alumina Alu C	0.1667
2-1	30	1400-850	Silica R974	Alumina Alu C	0.0535
2-1	60	1400-850	Silica R974	Alumina Alu C	0.0141
5-1	10	1400-850	Silica R974	Alumina Alu C	0.0280
5-1	30	1400-850	Silica R974	Alumina Alu C	0.0029
10-1	20	1400-850	Silica R974	Alumina Alu C	0.0035
10-1	30	1400-850	Silica R974	Alumina Alu C	0.0040

REFERENCES

1. Wei D, Dave RN, Pfeffer R. "Mixing and characterization of nanosized powders: An assessment of different techniques", Journal of Nanoparticle Research, 4 1-2, pp. 21-41, 2002.

2. Yang J, Wang Y, Dave RN, Pfeffer R. "Mixing of nano-particles by rapid expansion of high-pressure suspensions", Advanced Powder Technology, 14 (4), pp. 471-493, 2003.

3. Siegel RW. In: Siegel RW, Hu E. Reco MC eds. "Nanostructure Science and Technology: A Worldwide Study", WTEC, Loyola College in Maryland, pp. 1–14, 1999.

4. Roco MC. "Nanoparticles and nanotechnology research", Journal of Nanoparticle Res. 1(1), 1–6, 1999.

5. Carter SA, Scott JC, Broack PJ. "Enhanced luminance in polymer composite light emitting device", Appl. Phys. Lett., 71, 1145–1147, 1997.

6. Maser WK, Lukyanchuk I, Bernier P, Molini P, Lefrant S, Redlich P, Ajayan PM. "Superconducting RNi_2B_2C (R = Y, Lu) nanoparticles: size effects and weak links", Adv. Mater. 9, 503, 1997.

7. Imanaka N, Kohler J, Toshiyuki M. "Inclusions of nanometer-sized Al_2O_3 particles in a crystalline $(Sc,Lu)_2(WO_4)_3$ matrix", Journal of Am. Ceram. Soc. 83, 427–429, 2000.

8. Steyer P, Mege A, Pech D, Mendibide C, Fontaine J, Pierson J-F, Esnouf C, Goudeau P. "Influence of the nanostructuration of PVD hard TiN-based films on the durability of coated steel", Surface and Coating Technology, 2007. doi:10.1016/j.surfcoat.2007.08.073

9. Kaye BH. "Powder Mixing", Powder Technology Series, Chapman & Hall, pp. 19-35, 77–131, 1997.

10. Reddy V. "Getting from wet to dry", Manufacturing Engineering, 102 (6), pp. 83-86, (1989).

11. Ramlakhan M, Wu C-Y, Watano S, Dave RN, and Pfeffer R. "Dry particle coating using magnetically assisted impaction coating (MAIC): modification of surface properties and optimization of system and operating parameters" Powder Technology, 112, 137-148, 2000.

12. Danckwerts PV, "The definition and measurement of some characteristics of mixtures", Appl. Sci. Res. A3, pp. 279-296, 1952.

13. Barrow R, Yang J, Dave R, Pfeffer R. "Dry-mixing of sub-micron B and $BaCrO_4$ particles for use in a time delay composition", SAFE Journal, 35 (1), pp. 7-13, 2007.

14. Pfeffer R, Dave RN, Wei D, Ramlakhan M. "Synthesis of engineered particulates with tailed properties using dry particle coating", Powder Technology, 117, pp. 40-67, 2001.

15. Hendrickson W.A. & J. Abbott, 1999. US Patent: 5962082.

16. Singh RK, Ata A, Fitz-Gerald J, Hendrickson W. "Dry coating method for surface modification of particulates", In: Sudarshan TS, Khor KA, Jeandin M. eds. Surface Modification Technology X, The Institute of Materials, London, 1997.

17. Prausnitz J, Lichtenthaler RN, Gomes de Azevedo E. Molecular Thermodynamics of Fluid-Phase Equilibria. New Jersey: Prentice-Hall, 3rd Ed, 1999.

18. Castellanos A. "The relationship between attractive interparticle forces and bulk behaviour in dry and uncharged fine powders," Advances in Physics, 54, 263-376, 2005.

19. Rabinovich YI, Adler JJ, Ata A, Moudgil BM, Singh RK. "Adhesion between Nanoscale Rough Surfaces I. Role of Asperity Geometry", Journal of Colloid Interface Sci., 232, 10-16, 2000.

20. Rabinovich YI, Adler JJ, Esayanur MS, Ata A, Singh RK, Moudgil BM. "Capillary forces between surfaces with nanoscale roughness", Journal of Colloid Interface Sci., 232, 10-16, 2000.

21. Van der Wel, Peter G J. "Powder Mixing", Powder Handling Process., 11(1), pp. 83-86, 1999.

22. Peciar M, et al., "Mixing of finely powdered materials", Chem. Prum., 42(5-6), pp. 124-6, 1992.

23. Naganuma N, et al., "Mixing powder with liquid", Netsu Shori., 31(2), pp. 95-9, 1991.

24. Vaizoglu O, et al., "Assessment of the degree of mix of powder mixtures", Turk. J. Phys., 23(1), pp. 97-104, 1999.

25. Wightman C, et al., "Quantitative characterization of powder blending processes", AIChE Symp. Ser., 313, pp. 71-75, 1996.

26. Makino K, et al. "Development of simultaneous measurement of method for powder porosity and mixing ratio in mixing powder and its application", Sozai Busseigaku Zasshi., 3(2), pp. 72-83 1990.